

The University of San Francisco

USF Scholarship: a digital repository @ Gleeson Library | Geschke Center

Master's Theses

All Theses, Dissertations, Capstones and
Projects

Spring 5-18-2024

Downregulation of DAX-1 Expression via miRNA Overexpression as a Mechanism to Potentiate Breast Cancer

Nicholas C. DeVito
n.devito@tcu.edu

Follow this and additional works at: <https://repository.usfca.edu/thes>



Part of the [Biology Commons](#)

Recommended Citation

DeVito, Nicholas C., "Downregulation of DAX-1 Expression via miRNA Overexpression as a Mechanism to Potentiate Breast Cancer" (2024). *Master's Theses*. 1589.

<https://repository.usfca.edu/thes/1589>

This Thesis is brought to you for free and open access by the All Theses, Dissertations, Capstones and Projects at USF Scholarship: a digital repository @ Gleeson Library | Geschke Center. It has been accepted for inclusion in Master's Theses by an authorized administrator of USF Scholarship: a digital repository @ Gleeson Library | Geschke Center. For more information, please contact repository@usfca.edu.

**DOWNREGULATION OF DAX-1 EXPRESSION VIA miRNA OVEREXPRESSION AS
A MECHANISM TO POTENTIATE BREAST CANCER**

By

Nicholas Christopher DeVito

Thesis

Submitted in Partial Fulfillment of the Requirements
for the Degree of

**Master of Science
In Biology**

In The
College of Arts and Sciences
University of San Francisco
San Francisco, California

Committee in Charge

Approved:	 _____	<u>08/13/2024</u>
	<i>Dr. Christina Tzagarakis-Foster</i>	<i>Date</i>
Approved:	 _____	<u>8/15/2024</u>
	<i>Dr. Sangman Kim</i>	<i>Date</i>
Approved:	 _____	<u>08/13/2024</u>
	<i>Dr. Jennifer Dever</i>	<i>Date</i>

Abstract

The orphan nuclear receptor DAX-1 (Dosage Sensitive Sex Reversal, Adrenal Hypoplasia Congenita, critical region on the X chromosome, gene 1) plays a key role in mammalian sex determination and steroidogenesis. In addition to these canonical examples, DAX-1 has been shown to play a contradictory role in cancer development. While DAX-1 is overexpressed in lung and prostate cancer, it is downregulated in breast cancer. One of the explanations for the paradoxical role of DAX-1 in cancer development could be microRNA (miRNA) dysregulation. After broadly surveying over 96 miRNAs historically upregulated in MCF7 breast cancer cells, we compared the expression of DAX-1 in MCF7 and MCF10A (normal breast epithelial) cells with the presence of specific miRNA inhibitors. Our primary hypothesis remains that multiple miRNAs negatively regulate the expression of DAX-1 in human breast cancer cells and are not overexpressed in normal breast cells, providing another mechanism of lifting the repression of DAX-1 expression. Quantitative PCR and western blot analysis was performed indicating that miRNA-29b, 100, 199a, and 424 all downregulate DAX-1 expression. Similar techniques were explored to determine that miR-20b and miR-22 inhibition downregulates Estrogen Receptor α expression whereas miR-29b, 29c, and 424 inhibition indicates Cyclin D1 underexpression. Finally, we examined the migratory properties of MCF7 cells following miRNA inhibition via scratch-and-heal assays. This research will allow clinicians to screen for miRNAs that are elevated in BC patients substantially increasing the number of people diagnosed with breast cancer early on, and it will provide another method for diagnosing breast cancer or those who do not have access to preventative care.

Acknowledgements

First and foremost, I want to profusely thank my PI: Dr. Christina Tzagarakis-Foster. Dr. T, your guidance and mentorship has been invaluable and the true highlight of my graduate school experience here at USF. My abilities and confidence as a researcher has exponentially grown while in your lab. Thank you. Thank you. Thank you.

I would also like to thank my committee members Dr. Kim and Dr. Dever. Your support, suggestions, and edits have motivated me to make not only this work better but also me better as a scientist.

To the TRoEL Team:

Masters Students:

Lana Rasoul

Brandon Toy

Undergraduate Students:

Ayden Aloia

Shayla Caoile

Abby Chiang

Kalei Chin

Sadaf Dabiri

Anais Hernandez

Aarya Mishra

Sunaina Nayak

Alexander Osibin

You are all incredible! I especially want to thank Shaya, Abby, and Sadaf for all of their help with my qPCR and IncuCyte experiments.

I also want to express my gratitude to the Whitehead Fellowship and the USF Biology Department's Grant-In-Aid for their financial support which allowed me to work on this research during the Summer of 2023 and present my findings at the annual American Association for Cancer Research conference in April of 2024.

Finally, I want to dedicate this work to two members of my family. First, to my grandmother, Diane Clemens, a breast cancer survivor, who turned down a career in medicine to raise a family. Secondly, to my godfather, Christopher DeVito, who passed away, after a two year battle with pancreatic cancer, on May 4th, 2024. He was truly one of the most kind, just, and supportive people I have known.

Table of Contents

Abstract	2
Acknowledgments	3-4
Table of Contents	5-6
List of Figures	7-8
List of Tables	9
Abbreviations	10-12
Chapter 1: General Introduction	13-25
Breast Cancer.....	13-18
DAX-1.....	19-21
microRNA.....	21-24
Hypothesis and Specific Aims.....	25
Chapter 2: Dysregulatory miRNA Overexpression in Breast Cancer	26-38
Introduction.....	26-27
Methods.....	28-30
Results.....	31-37
Discussion.....	38
Chapter 3: Effect of miRNA Inhibition on DAX-1 Expression	39-50
Introduction.....	39
Methods.....	40-43
Results.....	44-47
Discussion.....	48-50
Chapter 4: Effect of miRNA Inhibition on ERα and CCND1 Expression	51-67
Introduction.....	51-52
Methods.....	53-56
Results.....	57-64
Discussion.....	65-67

Chapter 5: Effect of miRNA Inhibition on the Migratory Capabilities of MCF7 cells.....68-80
Introduction.....68
Methods.....69-71
Results.....72-79
Discussion.....80

Thesis Summary.....81-85

References.....86-92

List of Figures

Figure 1-1. Staging of BC.....	18
Figure 1-2. NHR Function.....	20
Figure 1-3. Protein Structure of Nuclear Hormone Receptors and DAX-1.....	21
Figure 1-4. miRNA Processing.....	23
Figure 2-1. miRNA Classification in BC.....	27
Figure 2-2. miRCURY LNA miRNA Focus PCR Panel Human Breast Cancer Plate Map.....	30
Figure 2-3 Upregulation of miRNA-106a in MCF7 cells.....	31
Figure 2-4. Differential miRNA Expression Panel in MCF7 and MCF10A Cells Assay 1.....	33
Figure 2-5. Differential miRNA Expression Panel in MCF7 and MCF10A Cells Assay 2.....	34
Figure 2-6. Differential miRNA Expression Panel in MCF7 and MCF10A Cells Assay 3.....	35
Figure 3-1. DAX-1 mRNA Expression in MCF7 Cells after miRNA Inhibitor treatment.....	44
Figure 3-2. DAX-1 Protein Expression in MCF7 Cells after miRNA Inhibitor treatment.....	45
Figure 3-3. DAX-1 mRNA Expression in MCF10A Cells after miRNA Inhibitor treatment.....	46
Figure 3-4. DAX-1 Protein Expression in MCF10A Cells after miRNA Inhibitor treatment.....	47
Figure 4-1. ER α mRNA Expression in MCF7 Cells after miRNA Inhibitor treatment.....	57
Figure 4-2. ER α Protein Expression in MCF7 Cells after miRNA Inhibitor treatment.....	58
Figure 4-3. ER α mRNA Expression in MCF10A Cells after miRNA Inhibitor treatment.....	59
Figure 4-4. ER α Protein Expression in MCF10A Cells after miRNA Inhibitor treatment.....	60
Figure 4-5. CCND1 mRNA Expression in MCF7 Cells after miRNA Inhibitor treatment.....	61
Figure 4-6. CCND1 Protein Expression in MCF7 Cells after miRNA Inhibitor treatment.....	62
Figure 4-7. CCND1 mRNA Expression in MCF10A Cells after miRNA Inhibitor treatment.....	63
Figure 4-8. CCND1 Protein Expression in MCF10A Cells after miRNA Inhibitor treatment.....	64

Figure 5-1. Sample Scratch of MCF7 cells.....	70
Figure 5-2. IncuCyte Plate Map.....	71
Figure 5-3. Scratch-and-heal Microscopy with KO miR-29c in MCF7 cells.....	72
Figure 5-4. Scratch-and-heal Microscopy with KO miR-199a in MCF7 cells.....	73
Figure 5-5. Scratch-and-heal Microscopy with KO miR-424 in MCF7 cells.....	74
Figure 5-6. Scratch-and-heal Microscopy with miR-Control Treatment in MCF7 cells.....	75
Figure 5-7. Scratch-and-heal Microscopy with TE Buffer Treatment in MCF7 cells.....	76
Figure 5-8. Wound Width over Time in MCF7 Cells Following miRNA Inhibition.....	77
Figure 5-9. Wound Confluence over Time in MCF7 Cells Following miRNA Inhibition.....	78
Figure 5-10. Relative Wound Density over Time in MCF7 Cells Following miRNA Inhibition.....	79
Figure 6-1. Diagram of miRNA Modulation of the DAX-1/ER α /CCND1 axis in MCF7 cells...	83

List of Tables

Table 1-1. The 5 Different Types of BC.....	14
Table 1-2. Risk Factors of BC.....	16
Table 1-3. The TNM Staging of BC.....	17
Table 1-4. The Stages (0-4) of BC.....	17
Table 2-1. List of Primers used for miRNA Specific qPCR.....	29
Table 2-2. List of Annealing Temperatures for miRNA Specific qPCR.....	29
Table 2-3. Thermal Cycler Conditions for miRNA Specific two-step Amplification qPCR.....	29
Table 2-4. List of miRNA Consistently and Significantly Upregulated in MCF7 Cells.....	36
Table 2-5. Literature Review of Differential miRNA Expression in BC.....	37
Table 3-1. List of miRCURY LNA™ miRNA Power Inhibitors.....	40
Table 3-2. List of Primers used for qPCR.....	41
Table 3-3. List of Annealing Temperatures for qPCR.....	41
Table 3-4. Thermal Cycler Conditions for two-step Amplification qPCR.....	42
Table 3-5. List of Antibodies used for Western Blotting.....	43
Table 4-1. miRCURY LNA™ miRNA Power Inhibitors.....	53
Table 4-2. List of Primers used for qPCR.....	54
Table 4-3. List of Annealing Temperatures for qPCR.....	55
Table 4-4. Thermal Cycler Conditions for two-step Amplification qPCR.....	55
Table 4-5. List of Antibodies used for Western Blotting.....	56
Table 5-1. miRCURY LNA™ miRNA Power Inhibitors	69

Abbreviations:

Ab - antibody

ACTB - beta actin

AGO - argonaute

AHC - Adrenal Hypoplasia Congenita

AR - androgen receptor

BC - breast cancer

BMRK - biomarker

BRCA1 - breast cancer type 1 susceptibility

BRCA2 - breast cancer type 2 susceptibility

CCND1 - Cyclin D1

CDK - cyclin dependent kinases

COL4A2 - collagen alpha-2(IV) chain

C1QTNF1 - complement C1q tumor necrosis factor-related protein 1

DAX-1- Dosage-Sensitive Sex Reversal, Adrenal Hypoplasia Congenita Critical Region,
chromosome X, gene 1

DCIS - Ductal Carcinoma in situ

DI - deionized

DNMTs - DNA methyltransferases

DSS - Dosage-Sensitive Sex Reversal

EMT - epithelial-mesenchymal transition

epi-miRs - miRNAs that target DNMTs

ER α - estrogen receptor alpha

ERE - estrogen response elements

E2 - estradiol

FOXA1 - forkhead box protein A1

GAPDH - Glyceraldehyde 3-phosphate dehydrogenase

HER2 - human epidermal growth factor 2

HR+ - hormone receptor-positive

hsa - human/Homo sapiens

KO - knockout

LN - lymph nodes

miRNA - microRNA

mRNA - messenger RNA

miR-C - Negative Control A

miR-20b - hsa-miR-20b-5p

miR-22 - hsa-miR-22-3p

miR-29b - hsa-miR-29b-3p

miR-29c - hsa-miR-29c-3p

miR-100 - hsa-miR-100-5p

miR-199a - hsa-miR-199a-3p

miR-424 - hsa-miR-424-5p

nM - nanomolar

NHR- nuclear hormone receptor

OncomiR - oncogenic miRNA

ONHR- orphan nuclear hormone receptor

PCDC4 - programmed cell death protein 4

PPAR γ - peroxisome proliferator-activated receptor gamma

PR - progesterone receptor

pRb - retinoblastoma protein

pre-miRNA - Preliminary miRNA

pri-miRNA - Primary miRNA

PTEN - phosphatase and tensin homologue

qPCR - quantitative PCR

RIPA - radioimmunoprecipitation assay buffer

RISC - RNA inducible silencing complex

RWD - Relative Wound Density

SPARC - secreted protein acidic and rich in cysteine

TNM - Tumor Number Metastasis

TSmiR - tumor suppressive miRNA

WB - Western Blot

WC - Wound Confluence

WW - Wound Width

UTR - untranslated regions

U6 - UniSp6

7HC - 7 hallmarks of cancer

CHAPTER 1:
GENERAL INTRODUCTION

Breast Cancer

Breast cancer (BC) is defined as a collection of malignancies that originate in the mammary tissue. Specifically, initial mutations arise in mammary cells bringing about uncontrolled cell growth, increased proliferation, and eventual metastasis culminating in BC. Since its first documentation in ancient Egypt, researchers and physicians have spent entire careers elucidating the mechanism of BC progression [1]. Emerging research in the last fifty years has correlated several important biological signaling pathways to BC development. The most well known of these pathways include mutations involving: human epidermal growth factor 2 (HER2), Estrogen Receptor (ER), and Progesterone Receptor (PR) [1]. While these pathways are vital for normal breast tissue formation, mutations render them overactive in many BC patients. On the other hand, some patients have triple negative BC where there is a lack of expression of any of the aforementioned receptors [1]. As is the case with many types of cancer, mutations in p53, a transcription factor that halts the cell cycle in response to DNA damage, and Ras, a small GTPase molecular switch that turns on cascades resulting in cell growth, differentiation, and survival, have also commonly been found in BC patients [2]. These infamous cancer causing mutations are generally categorized as either a tumor suppressor gene, such as p53, or as an oncogene like Ras. Furthermore, oncogenes refer to those genes whose alterations cause gain-of-function effects, while tumor suppressor genes cause loss-of-function effects that contribute to the malignant phenotype [2]. These protein mutations and the pathways they disable or constitutively activate contribute to BC being the second most common cancer-associated cause of death in women around the world [3]. Table 1-1 below is a summary of the 5 different types of BC.

Table 1-1 The 5 Different Types of BC

Ductal Carcinoma	<ul style="list-style-type: none"> ● Most common ● Forms in the lining of milk ducts ● Ductal Carcinoma in situ (DCIS)
Lobular Carcinoma	<ul style="list-style-type: none"> ● Cancer of the lobules (where milk is produced) ● Quickly spread to lymph nodes and milk ducts ● Relatively easy to treat
Triple Negative	<ul style="list-style-type: none"> ● PR, ER, and HER2 negative ● Aggressive and hard to treat ● More common in younger patients
Sarcoma	<ul style="list-style-type: none"> ● Cancer of connective tissue of the breast ● Relatively rare ● Ex. Phyllodes Tumor and angiosarcoma
Paget's Disease	<ul style="list-style-type: none"> ● Cancer of the areolar tissue ● Very rare ● Usually indicates underlying DCIS

In addition to these spontaneous mutations, there is also a genetic component to BC due to inherited mutations passed down from one generation to the next. Of all BC cases, these mutations result in approximately 10% of patients [4]. It is important to note that inherited mutations only predispose an individual to BC. A multitude of cascading events, more specifically additional mutations, must occur in order for individuals with hereditary and/or spontaneous mutations to develop BC. However, the rates of BC diagnosis increase to anywhere from 30-80% if an individual has 1 or more familial mutations [5]. The 2 most notable genes that have been studied extensively in BC patients are BRCA1 and BRCA2. These two genes encode 2 unrelated DNA repair proteins: breast cancer type 1 susceptibility (BRCA1) and breast cancer type 2 susceptibility (BRCA2) respectively. When a patient is BRCA1 or BRCA2 positive (+/+), they are considered “at risk” for developing breast cancer [5]. This discovery usually prompts healthcare professionals to screen for BC via mammography more frequently and earlier than the

typical once every other year and starting around 50 years old [6]. Moreover, some BRCA1 and BRCA2 +/- patients elect to receive yearly mammograms starting at age 25 [6]. In extreme cases, prophylactic bilateral mastectomy, the surgical removal of both breasts, is another preventative measure that has been found to reduce the incidence of BC by over 90% in patients with an inherited predisposing mutation [7]. The reason this practice does not prevent a cancer diagnosis is due not only to the likelihood of spontaneous mutations more likely to occur over time, but also the complex roles oncogenes play in additional cancers besides just breast [7]. Overall, a mastectomy or lumpectomy, the surgical removal of a lump in the breast, are the most effective methods to treat BC. However, chemotherapy, radiation and most recently immunotherapy are also viable treatment options depending on the patient and the tumor [7]. The previously stated causative factors of BC are the result of uncontrollable biological processes gone awry, but human behavior also plays a role in the likelihood of BC development [8,9]. The table below illustrates all of the known risk factors of BC.

Table 1-2 Risk Factors of BC [10]

Hormonal and reproductive	<ul style="list-style-type: none"> ● Early age of the first menstruation ● Late age of the last menstruation ● The first reported pregnancy at a late age (after 30 years of age) ● No pregnancies ● Postmenopausal condition ● Use of oral contraception ● Use of hormone replacement therapy
Physiological factors and health status	<ul style="list-style-type: none"> ● Older age (increased risk from 35 years of age) ● Family history of breast cancer ● Breast, ovarian and endometrial cancer in the past ● Occurrence of benign changes in the breasts,proceeding with the presence of atypical hyperplasia ● Ionizing radiation, used in connection with, for example,Hodgkin lymphoma therapy ● Rapid growth in adolescence and high growth in adulthood ● Infection with an oncogenic virus (e.g., Epstein–Barr)
Nutritional	<ul style="list-style-type: none"> ● Western type diet ● Excessive consumption of fats, especially animal fats ● High consumption of red and fried meat ● High iron intake ● Development of overweight/obesity after menopause ● Low consumption of fresh vegetables and fruits ● Low intake of phytoestrogens (isoflavones, lignans)
Other lifestyle-related	<ul style="list-style-type: none"> ● Regular moderate/high alcohol consumption ● Lack of regular physical activity ● Night work

Furthermore, BC tumors are organized and identified in two overlapping systems [11].

Table 1-3 The TNM Staging of BC

Letters	Explanation
T	Tumor size always in cm
N	Number of axillary Lymph Nodes with cancer
M	Metastasis has occurred (1) or has not occurred (0)

Table 1-4 The Stages (0-4) of BC

Stages	Description
Stage 0 (noninvasive)	Disease is exclusively in the ducts and lobules of the breast
Stage IA	Tumor is up to 2 cm in length and has not spread to the Lymph node
Stage IB	Tumor is less than 2 cm in length OR the tumor has spread to the Lymph node
Stage IIA	Tumor is 2-5 cm with or without invaded axillary Lymph node OR no tumor in breast but cancer cells in 1-3 axillary Lymph node
Stage IIB	Tumor is 2-5 cm and spread to 1-3 axillary Lymph node OR tumor is larger than 5 cm and has not spread to any Lymph node
Stage IIIA	Tumor is any size but has spread to more than 4 Lymph node
Stage IIIB (inflammatory BC)	Tumor is any size but has spread to the chest wall
Stage IIIC	Disease has spread to 10 or more axillary Lymph node
Stage IV (metastatic BC)	Disease has spread to other organs, tissues, and/or distant Lymph node

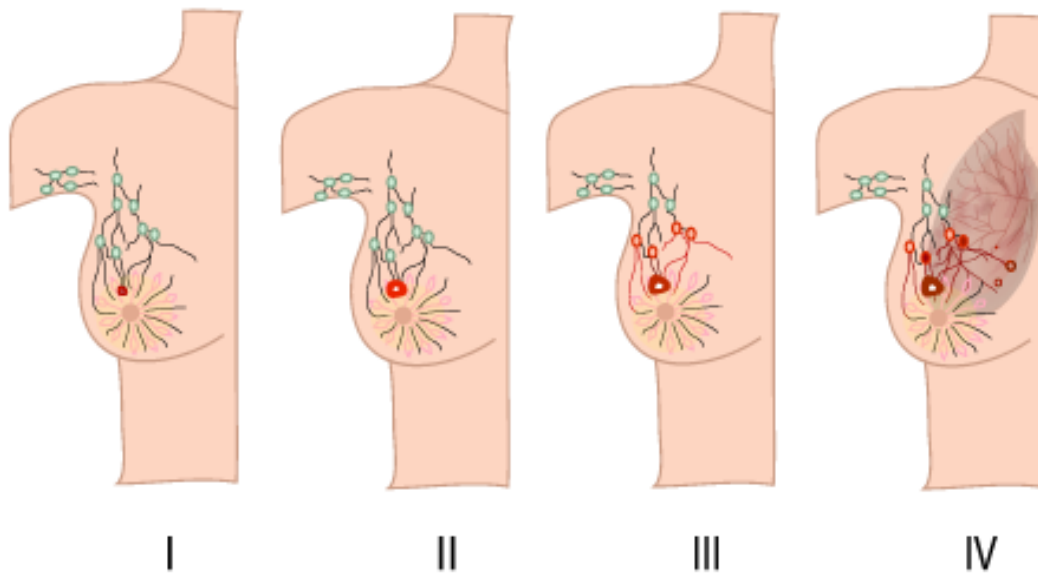


Figure 1-1. Staging of BC. Figure 1-1 illustrates the four main stages of BC. Stage I illustrates a local tumor that has not spread to any nearby LN. Stage II depicts a larger tumor with minimal or no LN involvement. Stage III highlights 4 axillary LN that have been invaded along with a large tumor. Stage 4 encapsulates metastatic BC with the invasion of lung tissue and distant LN. Besides the lung, BC commonly metastasizes in the brain, bone, and liver [11].

Currently, 13% of women will be diagnosed with BC in their lifetime [12]. As obesity rates continue to rise in the developed and developing world, BC rates, as well as the rates of other adipocyte driven cancers, will subsequently increase alongside them [12]. Besides reducing the instances of BC, the other main method for reducing BC related deaths and one of the primary objectives of this work remains to increase the number of BC patients diagnosed early.

DAX-1

Extensive research has been conducted in the Dr. Tzagarakis-Foster laboratory on the transcription factor DAX-1. Encoded by the NR0B1 gene, *DAX-1*, a member of the nuclear hormone receptor (NHR) family, is essential in the development of testes, ovaries, breast, and gonadal tissue and has wide regulatory effects on the synthesis of steroid hormones [13]. Mutations in the *DAX-1* gene are associated with X-linked adrenal hypoplasia congenita (AHC) and dosage-sensitive sex reversal (DSS). AHC is the result of a mutated nonfunctional copy of *DAX-1* and characterized by adrenal gland issues and hypogonadotropic hypogonadism [14]. DSS is due to a duplicate copy of *DAX-1* causing male to female sex reversal as these individuals appear female but are genetically male with both an X and Y chromosomes [15]. Besides pathogenesis, NHRs have a unique structure that enables them to influence a wide variety of genes. First, the N-terminal domain is crucial for activating transcription. In the middle of the protein, the DNA-binding domain binds to the target DNA sequence. Finally at the C-terminal end, a ligand-binding domain is necessary as NHRs depend on a ligand to function [16]. *DAX-1* belongs to a special subclass of NHRs known as orphan nuclear hormone receptors. Lacking a conserved intrinsic DNA-binding domain, *DAX-1* is a unique orphan receptor. In the absence of this domain, *DAX-1* acts as a regulator to suppress other NHRs and disrupt molecular pathways [17]. Besides mammalian sex determination and steroidogenesis, recent studies have highlighted the role of *DAX-1* in cancer.

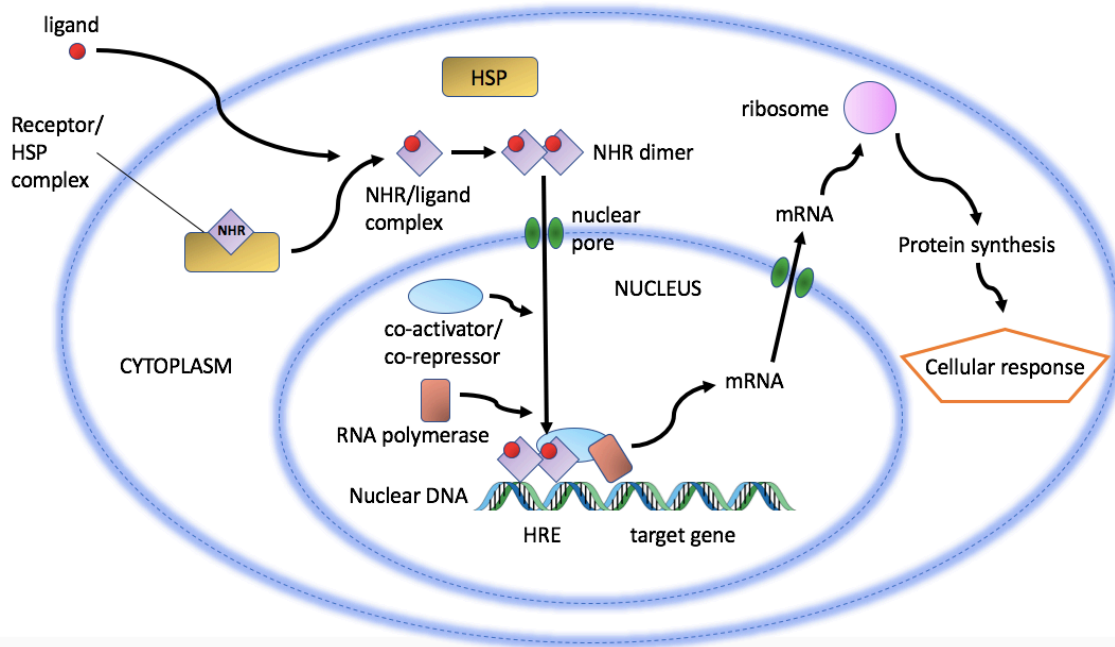


Figure 1-2. NHR Function. This schematic portrays the canonical NHR function inside the cell. First, a ligand enters the cytosol from outside the cell. Once bound, the NHR dimerizes and enters the nucleus. Here, co-activators/co-repressors and RNA polymerase directly bind to the DNA and influence transcription [18].

A.



B.

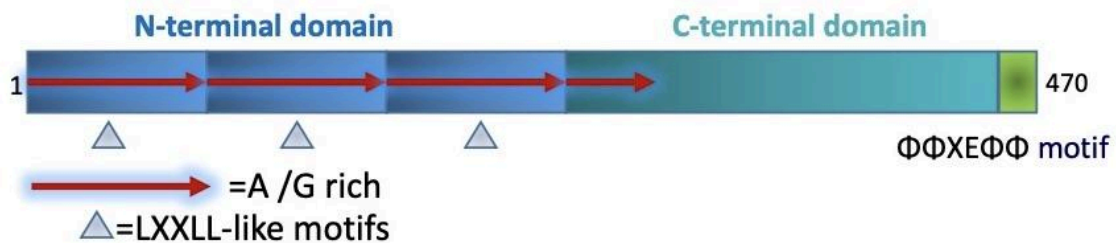


Figure 1-3. Protein Structure of Nuclear Hormone Receptors and DAX-1. **A)** The general schematic for NHR structure depicting an N-terminal domain (A/B), a DNA binding domain or DBD (C), a hinge region (D), a ligand binding domain or LBD (E), and a C-terminal domain (F). **B)** The protein structure of DAX-1 with 470 amino acid residues contains 3 alanine/glycine rich repeats and 3 LXXLL-like motifs on the N-terminal end, a 1/2 alanine/glycine rich repeat at the beginning of the C-terminal domain, and a $\Phi\Phi X E \Phi\Phi$ motif at the end of the C-terminal domain [19].

microRNA

miRNAs are small (18-23 nucleotides long) non-coding RNAs that have been shown to play a key role in a variety of diseases by silencing genes at the transcriptional level. miRNA originates as primary miRNA (pri-miRNA) that is anywhere from 300-1000 nucleotides long [20]. Pri-miRNA then folds into a structure known as “hairpin loops” and the ribonuclease Drosha/DGCR8 is able to cleave the pri-miRNA. Once cleaved, the pri-miRNA is transported out of the nucleus and into the cytoplasm by exportin 5. The pri-miRNA is classified as pre-miRNA, and is cleaved again by another ribonuclease: Dicer/TRBP. After this second cleavage, the pre-miRNA is denoted as mature miRNA [20]. At this point, the mature miRNA interacts with Argonaute proteins forming a RNA-induced silencing complex (RISC) [21]. miRNAs exert their influence on gene expression by binding to complementary sequences in the 3' untranslated regions (UTRs) of target messenger RNA (mRNA) molecules, thereby leading to mRNA degradation or translational repression. When a miRNA binds to the 3' UTR of its target mRNA with perfect or near-perfect complementarity, it can trigger mRNA degradation [21]. This process involves the recruitment of Argonaute proteins to the miRNA-mRNA complex. The interaction between the miRNA and its target mRNA leads to the recruitment of RISC, which contains the endonuclease activity that cleaves the mRNA, resulting in its degradation. As a consequence, the mRNA molecule is rapidly degraded, preventing its translation into protein [21]. In cases where the miRNA binds to the target mRNA with imperfect complementarity, translational repression occurs. In this mechanism, the miRNA-mRNA complex interferes with the translation process by blocking the binding of ribosomes or inhibiting translation initiation factors [23]. This prevents the mRNA from being translated into protein, effectively reducing the level of protein expression.

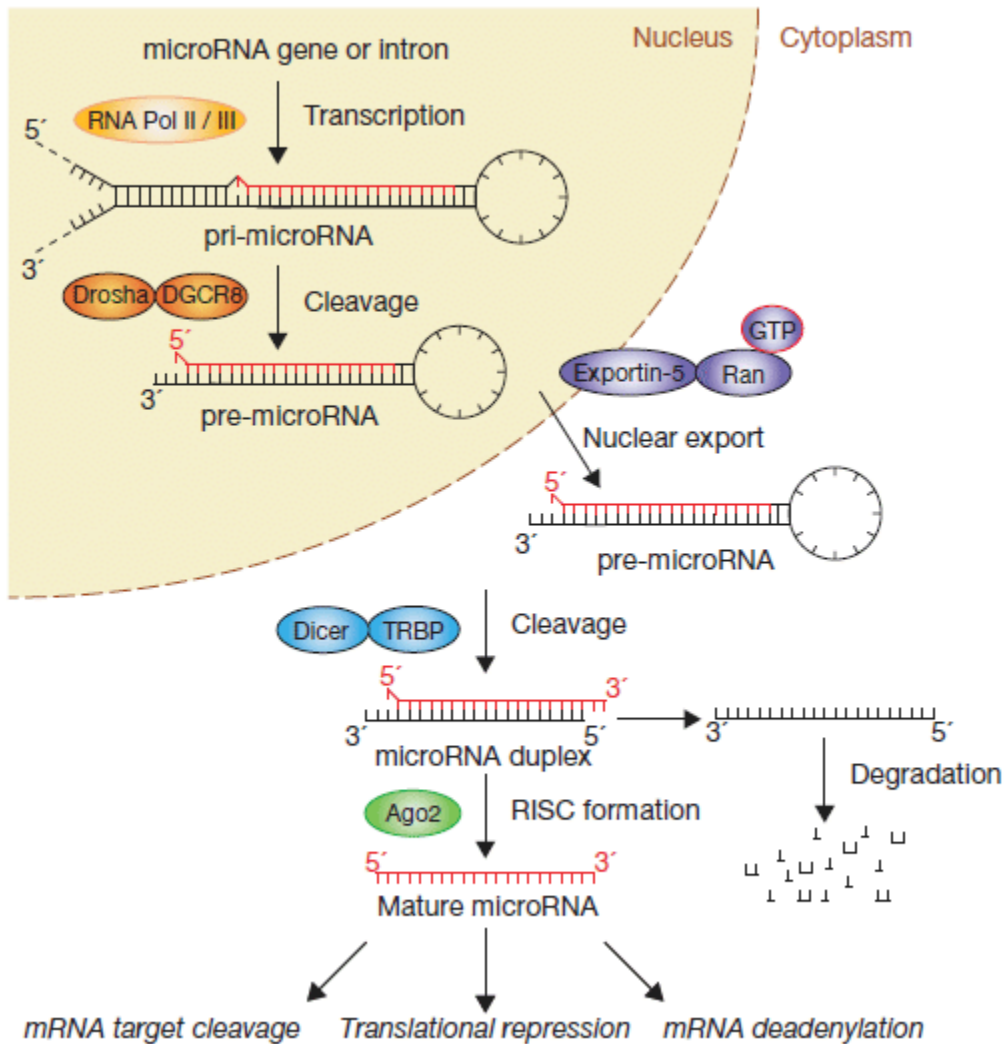


Figure 1-4. miRNA Processing. Figure 1-4 depicts the creation of miRNA including both cleavage partners: Drosha and Dicer as well as their binding partners. The end result of miRNA formation is the ability to downregulate protein expression via mRNA target cleavage, translational repression, or mRNA deadenylation [22].

As of 2024, approximately 3,600 miRNAs have been cataloged. Despite vast data being published in this new field, all of the mRNA targets of the identified miRNAs have yet to be determined. However, it is known that miRNAs repress over 60% of protein encoding genes [23]. This finding highlights the complexity of miRNA research in two distinct ways. Firstly, that miRNA are able to target more than one mRNA within the genome. Secondly, the same genes can be silenced by more than one miRNA. The interconnectedness pervasive in this phenomenon elicits over fifty million miRNA/mRNA pairings [22].

In cancer, miRNAs are classified in one of two ways. First, if the miRNA silences oncogenes they are denoted as tumor suppressive miRNA (TSmiR) [24]. Conversely, if the miRNA silences tumor suppressive genes they are classified as oncogenic miRNA (OncomiR). The classifications remain subjective and depend solely on the miRNA, mRNA target and cell type [24]. In BC, miRNA-21, miRNA-210, and miRNA-221 are drastically overexpressed in ER, PR, and HER2 -/- patients [25]. On the other hand, miRNA-10b, miRNA-145, and miRNA-205 are underexpressed [25]. Out of the 3,600 miRNA identified thus far, only one, miRNA-106a, has been observed to be overexpressed in BC and also downregulate DAX-1 expression. After inhibition of miRNA-106a, MCF7 cells' ability to proliferate, invade or metastasize was substantially decreased [26]. This experiment is functionally identical to an original 2014 study that examined the role of miRNA-181 in LNCaP (prostate cancer) cells. The authors found that miRNA-181 similarly downregulates *DAX-1* expression and is overexpressed in prostate cancer cells [27]. As of 2024, these are the only two miRNA that have been identified to downregulate DAX-1 and play a key role in the progression of cancer. One of the primary objectives of this thesis remains to identify additional miRNAs that downregulate *DAX-1* expression in BC.

Hypothesis

My primary hypothesis remains that multiple miRNAs downregulate the expression of DAX-1 in human breast cancer cells and are not overexpressed in normal breast cells, providing another mechanism of lifting the repression of DAX-1 expression.

Specific Aims:

1. Broadly survey miRNA expression in both MCF7 (breast cancer cell line) and MCF10A (non-malignant breast cells). Once a select few miRNA have been identified, inhibitors will be utilized to inactivate the miRNA in order to analyze the effect on *DAX-1* expression via qPCR and western blot .
2. Investigate genes associated with BC progression, ER α and Cyclin D1 via additional qPCR and Western blot analysis.
3. Analyze migratory and proliferative abilities via scratch-and-heal assays in the MCF7 cells with select miRNA inhibitor treatment.

CHAPTER 2:
DYSREGULATORY miRNA OVEREXPRESSION IN BREAST CANCER

INTRODUCTION:

miRNAs exert their influence on gene expression by binding to complementary sequences in the 3' untranslated regions (UTRs) of target messenger RNA (mRNA) molecules, thereby leading to mRNA degradation or translational repression [22]. Despite their modest size, miRNAs have profound effects on diverse biological processes, including development, differentiation, metabolism, and immune responses. Their dysregulation has been implicated in various diseases, including cancer, cardiovascular disorders, and neurodegenerative diseases, highlighting their potential as diagnostic markers and therapeutic targets [24]. By downregulating protein expression, certain miRNA are more potent than others due to the identity of their downstream targets. In cancer, these target genes often play a role in the seven hallmarks of cancer. The seven hallmarks of cancer include angiogenesis, invasion, migration, metastasis, uncontrolled proliferation, evading apoptosis, and inflammation [28]. Interestingly, certain miRNA are able to target more than one of these hallmarks [25]. This targeting by miRNA is summarized in the figure below with each miRNA classified as a TsmiR or an OncomiR. Overall, by elucidating which miRNA are significantly overexpressed in MCF7 cells compared to MCF10A, I was able to highlight possible miRNA that could target DAX-1 leading to BC progression.

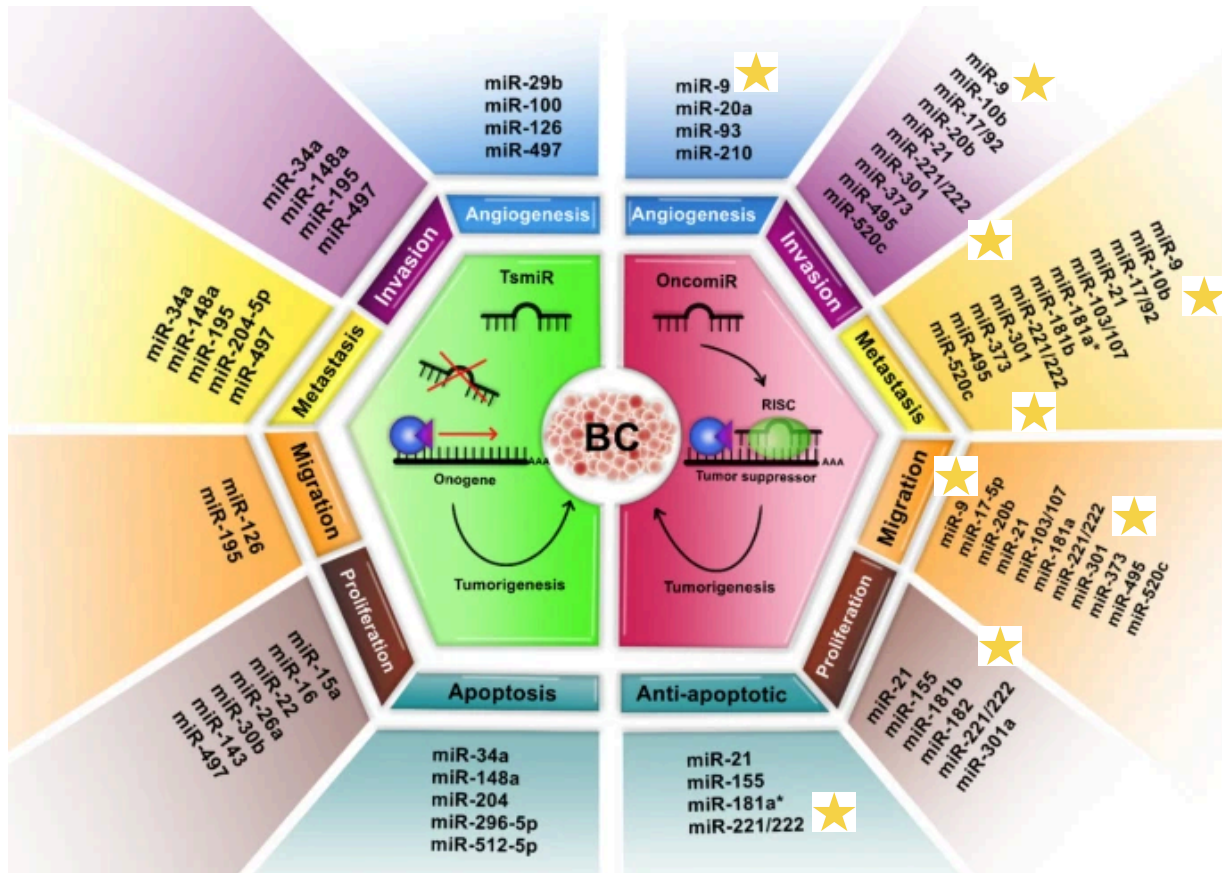


Figure 2-1. MiRNA Classification in BC. A summary of miRNA upregulated in BC. Notably, some miRNA play a role across several 7HC such as miRNA-9 and miRNA-221/222 [29].

★ - indicates miRNA-9 or miRNA-221/222

METHODS:

Cell Culture

All cells used in these experiments were stored in an incubator set to 37°C and 5% carbon dioxide. The cells were passaged every three days with MCF7 and MCF10A cells in DMEM and MEGM SingleQuots™ Supplement Pack (Lonza, Basel, Switzerland) media respectively. The media was purchased from ThermoFischer. DMEM was sustained with 50 milliliters of FBS and 5% PenStrep. MCF10A received 50 milliliters of FBS and additional media supplements (Lonza, Basel, Switzerland).

RNA Isolation, Purification and Quantification

First, total RNA was collected and purified using the Monarch Nucleic Acid Purification Kit (New England Biolabs, Inc Ipswich, MA). The protocol provided by the manufacturer was followed including the addition of the optional washes. Next, the isolated RNA was quantified and stored in a -80°C freezer.

miRNA specific Reverse Transcription

Qiagen miRCURY LNA RT Kit was used to perform reverse transcription on the quantified RNA. The protocol was followed identically with the optional Unisp6 template Spike-In included as well. The cDNA was stored in a -20°C freezer until used in downstream reactions.

miRNA specific qPCR

Qiagen miRCURY LNA qPCR Kit was used to complete the miRNA specific qPCR. The manufacturer's provided protocol was followed exactly. For a reference gene, the Unisp6 (U6) was used as the "control miRNA" as it is endogenous in cancer cell lines.

Table 2-1. List of primers used for miRNA specific qPCR

Primer	Forward Sequence (5' → 3')	Reverse Sequence (5' → 3')
miRNA-106a	AAAAGTGCTTACAGTGCAGGTAG	N/A
U6	CGCAAGGATGACACGCAAATTC	N/A

Table 2-2. List of Annealing Temperatures for miRNA Specific qPCR

Primer	Annealing Temperature qPCR
miRNA-106a	56°C
U6	56°C

Table 2-3. Thermal Cycler Conditions for miRNA Specific two-step Amplification qPCR

Step	Temperature	Time
Initial Denaturation	95°C	2 minutes
40 Cycles:		
Denaturation	95°C	10 seconds
Annealing	56°C	1 minute
+Plate Read		
Hold	4°C	∞

miRNA BC panel assay

The miRCURY LNA miRNA Focus PCR Panel Human Breast Cancer Focus V2 (Qiagen Venlo, Netherlands,) was purchased and the directions were completed exactly as stated in the manufacturer's instructions. The panel was performed twice per cell line (MCF7 and MCF10A). Figure 2-2 below depicts the plate map used for each round of the assay.

	1	2	3	4	5	6	7	8	9	10	11	12
A	hsa-let-7a-5p	hsa-let-7b-5p	hsa-let-7c-5p	hsa-let-7d-5p	hsa-let-7e-5p	hsa-let-7f-5p	hsa-let-7g-5p	hsa-let-7i-5p	hsa-miR-1-3p	hsa-miR-100-5p	hsa-miR-107	hsa-miR-10a-5p
B	hsa-miR-10b-5p	hsa-miR-125b-5p	hsa-miR-125b-1-3p	hsa-miR-128-3p	hsa-miR-129-5p	hsa-miR-130a-3p	hsa-miR-130b-3p	hsa-miR-132-3p	hsa-miR-140-5p	hsa-miR-141-3p	hsa-miR-145-5p	hsa-miR-148a-3p
C	hsa-miR-152-3p	hsa-miR-155-5p	hsa-miR-15a-5p	hsa-miR-15b-5p	hsa-miR-16-5p	hsa-miR-17-5p	hsa-miR-181a-5p	hsa-miR-181b-5p	hsa-miR-181c-5p	hsa-miR-181d-5p	hsa-miR-182-5p	hsa-miR-186-5p
D	hsa-miR-18a-5p	hsa-miR-193b-3p	hsa-miR-195-5p	hsa-miR-199a-3p	hsa-miR-199a-5p	hsa-miR-19a-3p	hsa-miR-19b-3p	hsa-miR-200a-3p	hsa-miR-200b-3p	hsa-miR-200c-3p	hsa-miR-202-3p	hsa-miR-203a-3p
E	hsa-miR-204-5p	hsa-miR-205-5p	hsa-miR-206	hsa-miR-20a-5p	hsa-miR-20b-5p	hsa-miR-21-5p	hsa-miR-210-3p	hsa-miR-212-3p	hsa-miR-214-3p	hsa-miR-22-3p	hsa-miR-222-3p	hsa-miR-223-3p
F	hsa-miR-25-3p	hsa-miR-26a-5p	hsa-miR-26b-5p	hsa-miR-27a-3p	hsa-miR-27b-3p	hsa-miR-29a-3p	hsa-miR-29b-3p	hsa-miR-29c-3p	hsa-miR-31-5p	hsa-miR-328-3p	hsa-miR-340-5p	hsa-miR-424-5p
G	hsa-miR-429	hsa-miR-485-5p	hsa-miR-489-3p	hsa-miR-495-3p	hsa-miR-497-5p	hsa-miR-548c-3p	hsa-miR-607	hsa-miR-613	hsa-miR-7-5p	hsa-miR-93-5p	hsa-miR-96-5p	hsa-miR-98-5p
H	cel-miR-39-3p	cel-miR-39-3p	SNORD44 (hsa)	SNORD38B (hsa)	SNORD49A (hsa)	U6 snRNA (v2)	UniSp2	UniSp4	UniSp5	UniSp6	UniSp3 IPC	UniSp3 IPC

Figure 2-2. miRCURY LNA miRNA Focus PCR Panel Human Breast Cancer Plate Map.

This plate map shows the exact primer for each specific miRNA by well. All 96 wells were used in every experiment.

RESULTS:

miRNA-106a upregulation in MCF7 cells

Preliminary qPCR analyzing miRNA-106a expression in MCF7 and MCF10A cells in order to validate the methods for multiple assays (Figure 2-3).

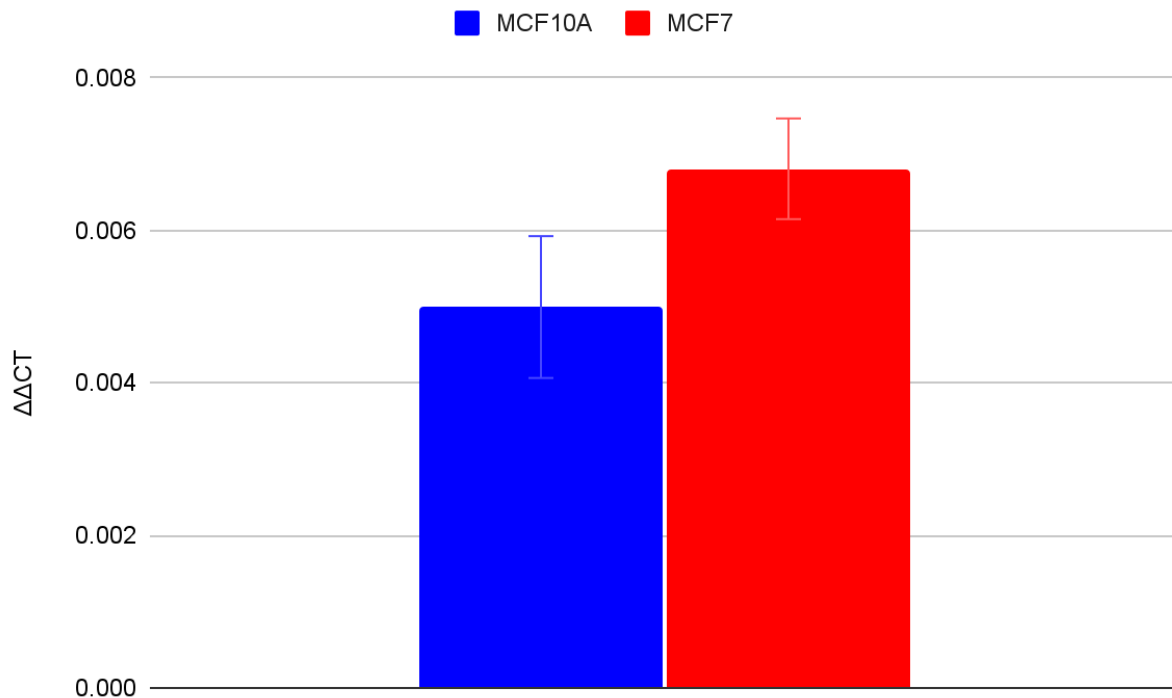


Figure 2-3. Upregulation of miRNA-106a in MCF7 cells. qPCR results showing fold-change expression of miRNA-106a in MCF7 and MCF10A cells. U6 was used as a control and experimental genes were compared to U6 as a baseline. Fold-change values were calculated by comparing both cell lines following the $\Delta\Delta CT$ method. Error bars on qPCR results represent the standard deviation of the mean for each sample run in triplicate.

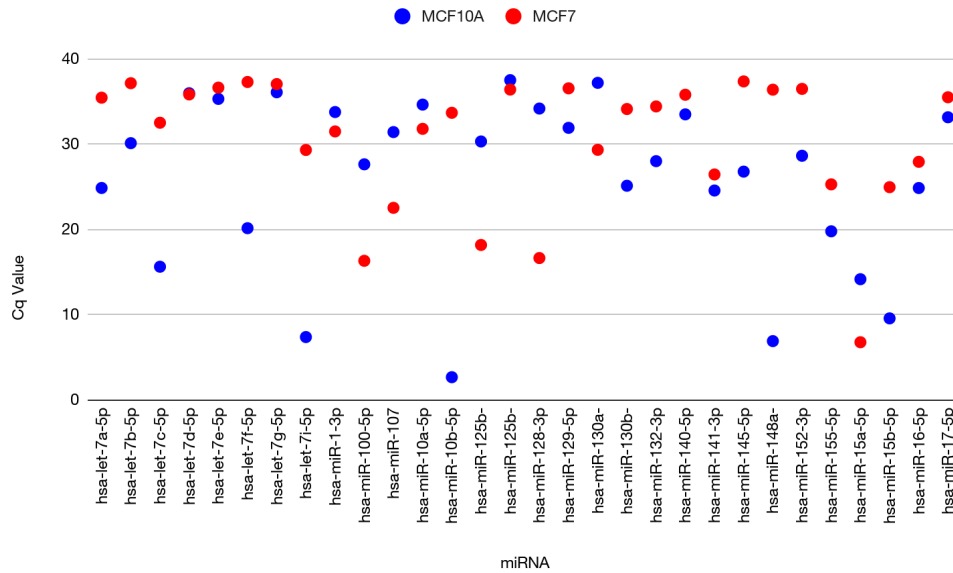
$$\Delta\Delta CT = 2^{-(\text{AVG of Target Gene } C_q - \text{AVG of Reference Gene } C_q)}$$

$$\text{STDEV} = \sigma = \sqrt{\frac{\sum(x_i - \mu)^2}{N}}$$

miRNA dysregulation in MCF7 cells

After initial qPCR data validated the miRNA specific cDNA synthesis and qPCR analysis, subsequent assays were completed highlighting the different miRNA expression in MCF7 and MCF10A cells. The panel was repeated twice for both cell lines. The Cq value on the y axis corresponds to the amount of miRNA expression. The data is divided into three different assays (Figure 2-4, 2-5, 2-6) shown below with 30, 38, and 28 miRNAs examined respectively.

A



B

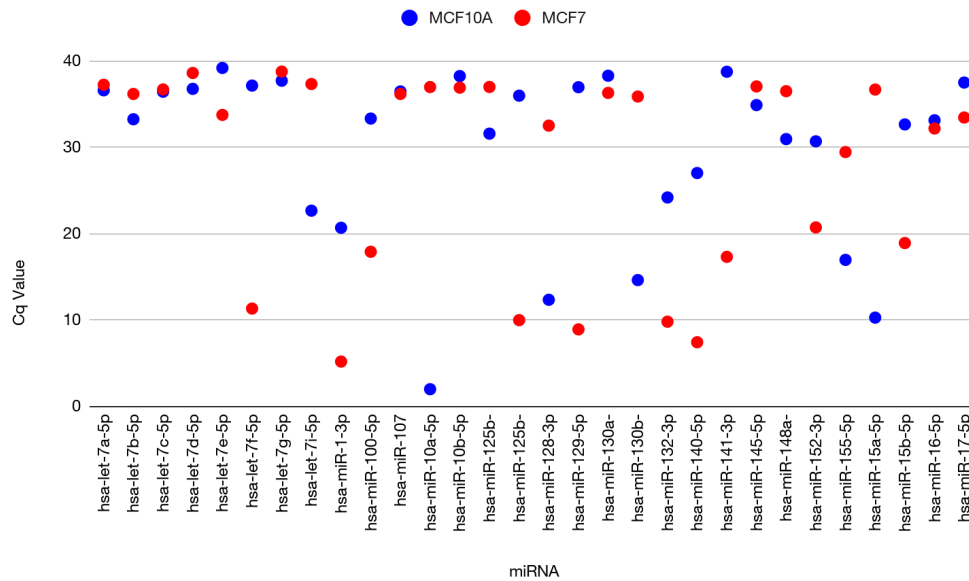
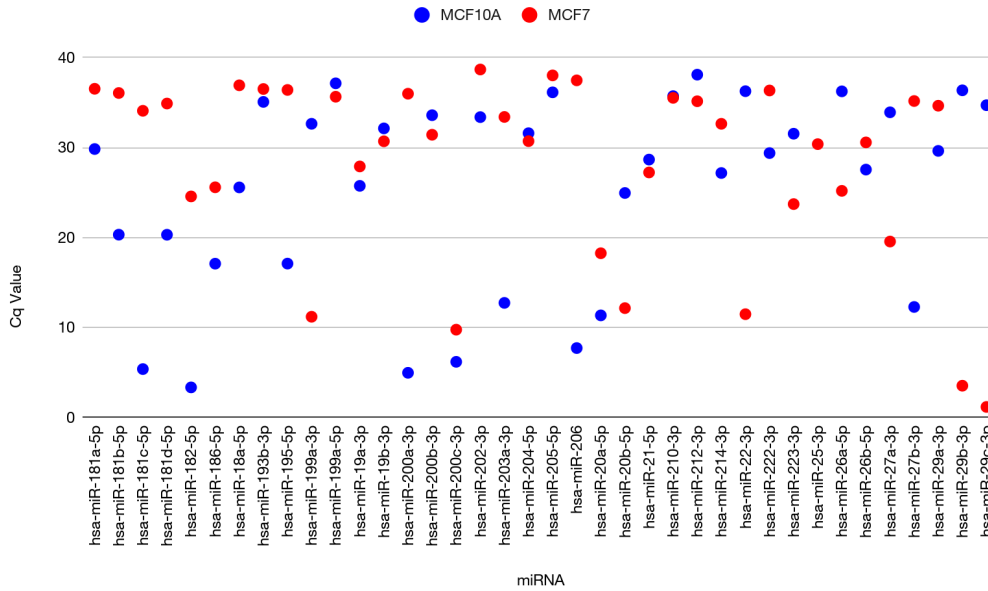


Figure 2-4. Differential miRNA Expression Panel in MCF7 and MCF10A Cells Assay 1.

qPCR results depict varying Cq expression of miRNA in MCF7 (red circles) and MCF10A (blue circles) cells. **A)** qPCR data from the first trial while **B)** is qPCR data from the second.

A



B

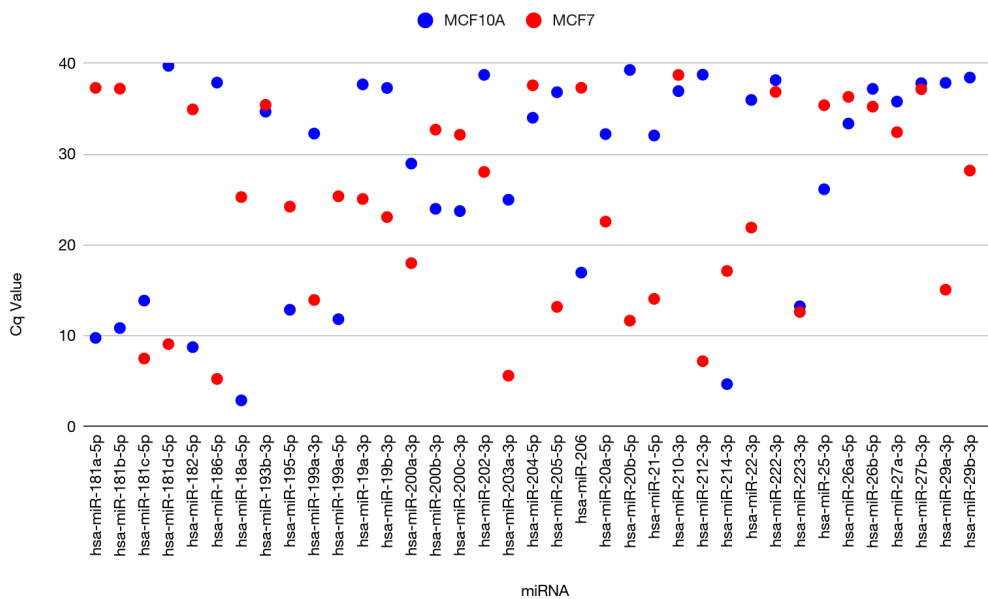
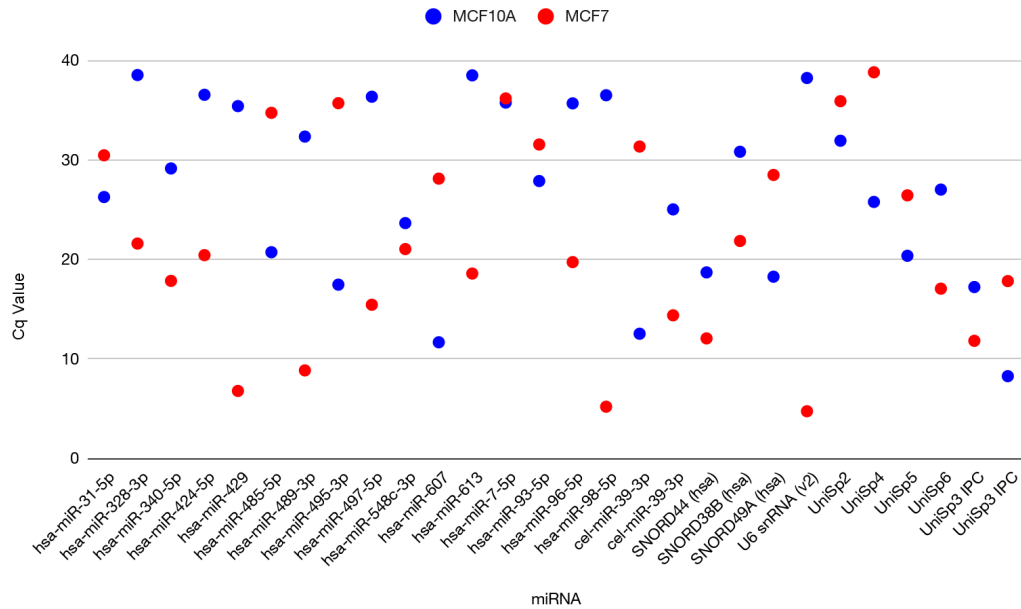


Figure 2-5. Differential miRNA Expression Panel in MCF7 and MCF10A Cells Assay 2.

qPCR results depict varying Cq expression of miRNA in MCF7 (red circles) and MCF10A (blue circles) cells. **A)** qPCR data from the first trial while **B)** is qPCR data from the second.

A



B

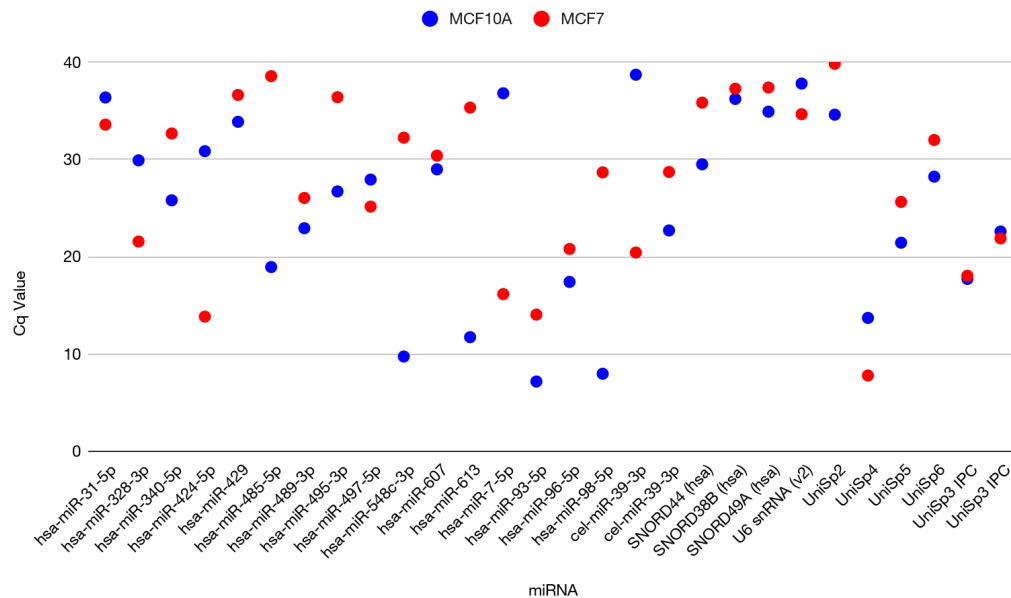


Figure 2-6. Differential miRNA Expression Panel in MCF7 and MCF10A Cells Assay
3.qPCR results depict varying Cq expression of miRNA in MCF7 (red circles) and MCF10A (blue circles) cells. A) qPCR data from the first trial while B) is qPCR data from the second.

After raw Cq data was obtained, statistical analysis was performed in order to elucidate not only which miRNA were upregulated in MCF7 cells for both panels but also eliminate any miRNA that did not have a differing Cq value greater than 10. In other words, The Cq value of a specific miRNA had to be < 10 than its MCF10A counterpart across both panels. After this analysis was performed, only 7 miRNA were identified (Table 2-4). The 5p/3p nomenclature is shorthand for denoting which side of the pre-miRNA did the mature miRNA originate from. Specifically, 5p is the 5' end and 3p is the complimentary 3' end. Additionally, for the remainder of this thesis hsa (human) will be assumed.

Table 2-4. List of miRNA Consistently and Significantly Upregulated in MCF7 Cells

miRNA	miRNA Sequence (5' → 3')
hsa-miR-20b-5p (miR-20b)	CAAAGUGCUCUAUAGUGCAGGUAG
hsa-miR-22-3p (miR-22)	AAGCUGCCAGUUGAAGAACUGU
hsa-miR-29b-3p (miR-29b)	UAGCACCAUUUGAAAUCAGUGUU
hsa-miR-29c-3p (miR-29c)	UAGCACCAUUUGAAAUCGGUUA
hsa-miR-100-5p (miR-100)	AACCCGUAGAUCCGAACUUGUG
hsa-miR-199a-3p (miR-199a)	ACAGUAGUCUGCACAUUGGUUA
hsa-miR-424-5p (miR-424)	CAGCAGCAAUUCAUGUUUUGAA

Table 2-5. Literature Review of Differential miRNA Expression in BC.

miRNAs Differentially Expressed	Source Citation
29c, 199a, 100, 29b, 22, 20b, 424	[30]
29c, 100, 22, 199a, 20b, 424	[31]
29c, 100, 29b, 20b, 22	[32]
100, 29b, 22, 20b	[33]
100, 29b, 22, 199a, 20b, 424	[34]
100, 22, 424, 20b, 199a	[35]
100, 22, 20b, 199a, 424	[36]
29c, 100, 29b, 20b, 424	[37]
29c, 29b, 100	[38]
100, 29b, 199a, 22	[39]
100, 29b, 29c	[40]
100, 424	[41]
29c, 100, 29b, 22, 424	[42]
100, 199a	[43]
22, 100, 29b, 29c	[44]
100, 199a	[45]
29c, 100	[46]
100	[47]
22, 100,	[48]
29c	[49]
29c, 100	[50]
29c	[51]
100	[52]
100	[53]
22, 100	[54]
22	[55]
29c	[56]
29c	[57]
29b	[58]
20b	[59]

DISCUSSION:

miRNAs directly regulate gene expression, and are frequently dysregulated in BC, contributing to disease initiation, progression, and metastasis. Upregulation of certain miRNAs in BC has been extensively studied and is associated with diverse biological processes implicated in tumorigenesis [25]. Several miRNAs are consistently upregulated in BC across different subtypes and stages of the disease. The upregulation of specific miRNAs in BC is often associated with poor clinical outcomes, including shorter overall survival, increased risk of recurrence, and resistance to chemotherapy [25]. After surveying 96 miRNA historically upregulated in BC, 7 miRNA were found to be significantly upregulated in MCF7 cells compared to MCF10A cells by qPCR (Table 2-4). Similar findings were reported in a comprehensive literature review (Table 2-5). Notably, there is approximately equal published literature documenting downregulation of miRNA in BC as there is stating observed overexpression. Understanding the mechanisms underlying the shift from endogenous miRNA expression to dysregulation in BC is crucial in order to create miRNA signatures. These signatures or panels can serve as potential biomarkers for BC detection, classification, and prediction of treatment response [25].

The remainder of this thesis will focus on the 7 miRNA from Table 2-4. While data has shown any of these 7 miRNA could be downregulated or upregulated in specific subtypes and stages of disease (Table 2-5), the data and subsequent analysis from Figures 2-4, 2-5, and 2-6 illustrate significant miRNA upregulation in MCF7 cells compared to the MCF10A.

CHAPTER 3:
EFFECT OF miRNA INHIBITION ON DAX-1 EXPRESSION

INTRODUCTION:

The link between DAX-1 and BC is new territory in the field of oncologic developments. Previous research in the Tzagarakis-Foster laboratory identified reduced DAX-1 expression in hormone receptor-positive (ER and PR) patients [18]. Moreover, when MCF7 cells were transfected with DAX-1, proliferation and cell cycle protein expression decreased. Additionally, DAX-1 expression was downregulated in BC patients regardless of human epidermal growth factor receptor 2, estrogen receptor, or progesterone receptor status [18]. In order to assess the effect of miRNA inhibition on DAX-1 expression, inhibitors were purchased for the 7 aforementioned miRNA that were upregulated in MCF7 cells (Table 2-4). These inhibitors encapsulate the miRNA preventing it from binding and essentially inactivating them or knocking them out (KO). Since DAX-1, as an orphan nuclear receptor, has no known ligand, miRNA could be one method for DAX-1 repression in BC. The data in this chapter not only aligns with previous data indicating that DAX-1 is downregulated in BC but also elucidates a possible miRNA-driven mechanism for the downregulation of DAX-1 in ER positive BC.

METHODS:*Cell Culture*

All cells used in these experiments were stored in an incubator set to 37°C and 5% carbon dioxide. The cells were passaged every three days with MCF7 and MCF10A cells in DMEM and MEGM SingleQuots™ Supplement Pack (Lonza, Basel, Switzerland) media respectively. The media was purchased from Thermofischer. DMEM was sustained with 50 milliliters of FBS and 5% PenStrep. MCF10A received 50 milliliters of FBS and additional media supplements (Lonza, Basel, Switzerland).

miRNA inhibitor

Once the MCF7 and MCF10a cells reach confluency, miRCURY LNA™ miRNA Power Inhibitors (Qiagen, Venlo Netherlands) were used in order to knockdown the specific miRNA. The protocol was followed closely and cell lysate was collected following a 72 hour incubation. The inhibitors were consistently added at a concentration of 500 nM and TE buffer was used for the vehicle control.

Table 3-1. List of miRCURY LNA™ miRNA Power Inhibitors

miRNA inhibitors	Sequence (5' → 3')	Company
hsa-miR-20b-5p	ACCTGCACTATGAGCACTTT	QIAGEN, Venlo, Netherlands
hsa-miR-22-3p	CAGTTCTTCAACTGGCAGCT	QIAGEN, Venlo, Netherlands
hsa-miR-29b-3p	ACTGATTTCAAATGGTGCT	QIAGEN, Venlo, Netherlands
hsa-miR-29c-3p	CCGATTTCAAATGGTGCT	QIAGEN, Venlo, Netherlands
hsa-miR-100-5p	ACAAGTTCGGATCTACGGGT	QIAGEN, Venlo, Netherlands
hsa-miR-199a-3p	AACCAATGTGCAGACTACTG	QIAGEN, Venlo, Netherlands
hsa-miR-424-5p	AAACATGAATTGCTGCT	QIAGEN, Venlo, Netherlands
Negative Control A (miR-C)	TAACACGTCTATACGCCCA	QIAGEN, Venlo, Netherlands

Reverse Transcription

The qScript™ cDNA SuperMix kit (Quantabio, Beverly, MA) was used to synthesize cDNA from the isolated RNA. The concentration for all cDNA synthesis was 400nM and the directions were completed according to the manufacturer's instructions.

Quantitative PCR

cDNA synthesized from extracted mRNA was used as a template for qPCR. qPCR reactions were performed in triplicate using the BioRad CFX96 Real-Time PCR system (BioRad, Hercules, CA) qPCR reactions were prepared using 10 μ L of SYBR Green Master Mix (Life Technologies, Carlsbad, CA) or QuantiTect SYBR Green PCR kit (Qiagen, Venlo, Netherlands), 0.5 μ L of 10 μ M forward and reverse primers, 7.5 μ L of dH₂O, and 2 μ L of cDNA. Primers specific to the GAPDH housekeeping gene were used as a positive control and experimental genes were compared to GAPDH as a baseline. 100 μ M primers for DAX-1 and GAPDH were both diluted 1:10. The $\Delta\Delta$ CT method was used to calculate gene expression and the error bars on qPCR results represent standard deviation of the mean.

Table 3-2. List of Primers used for qPCR

Primer	Forward Sequence (5' → 3')	Reverse Sequence (5' → 3')
DAX-1	TCCGCGCCCTTGCCCAGACC	GCCGCACGAACAGCCCCAACACT
GAPDH	CCATCACCATCTTCCAGGAGCC	AGAGATGATGACCCTTTTGGC

Table 3-3. List of Annealing Temperatures for qPCR

Primer	Annealing Temperature qPCR
DAX-1	60°C
GAPDH	59°C

Table 3-4. Thermal Cycler Conditions for two-step Amplification qPCR

Step	Temperature	Time
Initial Denaturation	95°C	2 minutes
50 Cycles: Denaturation Annealing +Plate Read	95°C 60°C	15 seconds 1 minute
Hold	4°C	∞

Protein Isolation and Quantification

For protein isolation, cells were washed twice in ice cold 1X PBS and lysed in RIPA lysis buffer (25 mM Tris•HCl pH 7.6, 150 mM NaCl, 1% NP-40, 1% sodium deoxycholate, 0.1% SDS) including Halt Protease Inhibitors (Thermo Fisher, Waltham, MA) for 15 minutes at 4°C. Following cell lysis, the lysate was sonicated or passed through a syringe with a 21-gauge needle 4-5 times to breakdown genomic DNA and facilitate protein isolation. Sonicated lysates were centrifuged at 14,000 rpm, for 15 minutes at 4°C and the supernatant was transferred to a new microcentrifuge tube. After isolation, the protein samples were quantified using a BCA assay and stored in a -80°C freezer.

Western Blot

Equivalent amounts of various cell lysates were prepared including LDS Sample Buffer and 10X reducing agent (Thermo Fisher, Waltham, MA) that was compatible with the NuPAGE electrophoresis system. Samples were electrophoresed through a 10% SDS-PAGE gel and wet transferred for 1 hour to a PVDF membrane for blotting. Blots were washed with DI water twice, before a 10 minute incubation at room temperature in the SuperSignal™ Western Blot Enhancer Antigen Pretreatment Solution (Thermo Fisher, Waltham, MA), 5 DI water washes were performed before blots were blocked for 60 minutes at room temperature with 10% Bovine Serum Albumin in 1X TBS with 0.1% Tween (1X TTBS). Following blocking, and 1X TTBS washes, primary antibody was added to each blot in the SuperSignal™ Western Blot Enhancer Primary Antibody (Thermo Fisher, Waltham, MA) Diluent and incubated overnight at 4°C with rocking. 1:500 dilutions were used for the DAX-1 antibody while 1:1000 were used for β -actin. The following day, blots were washed with 1X TTBS and incubated with either anti-rabbit or anti-mouse secondary antibody (diluted 1:2000 in blocking solution) for 60 minutes at room temperature with rocking. Blots were washed with 1X TTBS and chemiluminescent (Azure Biosystems, Dublin, CA) detection of proteins will be performed using the GelDoc Imaging System (BioRad, Hercules, CA).

Table 3-5. List of Antibodies used for Western Blotting

Protein	Species	Company	Dilution Factor
DAX-1	Mouse (Monoclonal)	Active Motif, Carlsbad, CA	1:500
ACTB	Mouse (Monoclonal)	Thermo Fisher, Waltham, MA	1:1000

RESULTS

DAX-1 gene expression following miRNA inhibitor treatment in MCF7 cells

After miRNA inhibitor treatment, RNA isolation, and cDNA synthesis qPCR was performed in order to assess the effect of miRNA inhibition on DAX-1 gene expression in MCF7 cells. GAPDH was used as the control gene.

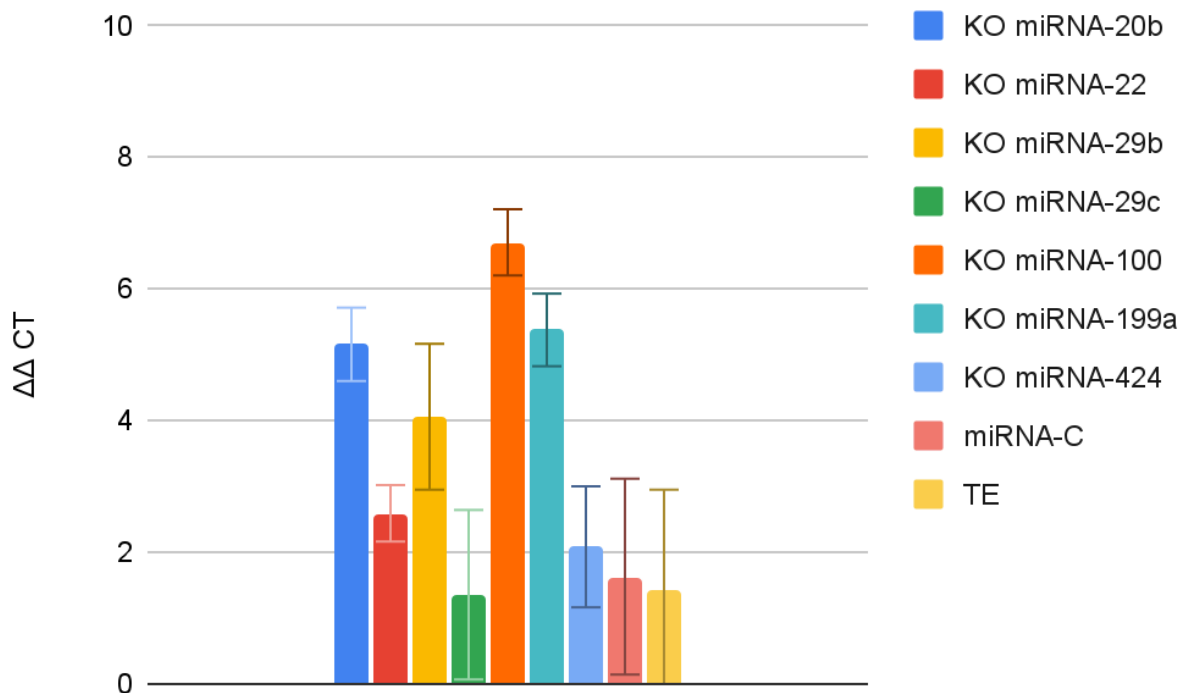


Figure 3-1. DAX-1 mRNA Expression in MCF7 Cells after miRNA Inhibitor treatment.

qPCR results depicting DAX-1 gene expression levels. Fold changes were calculated by $\Delta\Delta CT$ analysis normalized against GAPDH. Error bars represent standard deviation of the mean.

DAX-1 protein expression following miRNA inhibitor treatment in MCF7 cells

After miRNA inhibitor treatment and protein isolation, a western blot was performed in order to assess the effect of miRNA inhibition on DAX-1 protein expression in MCF7 cells. β -actin was used as the reference protein.

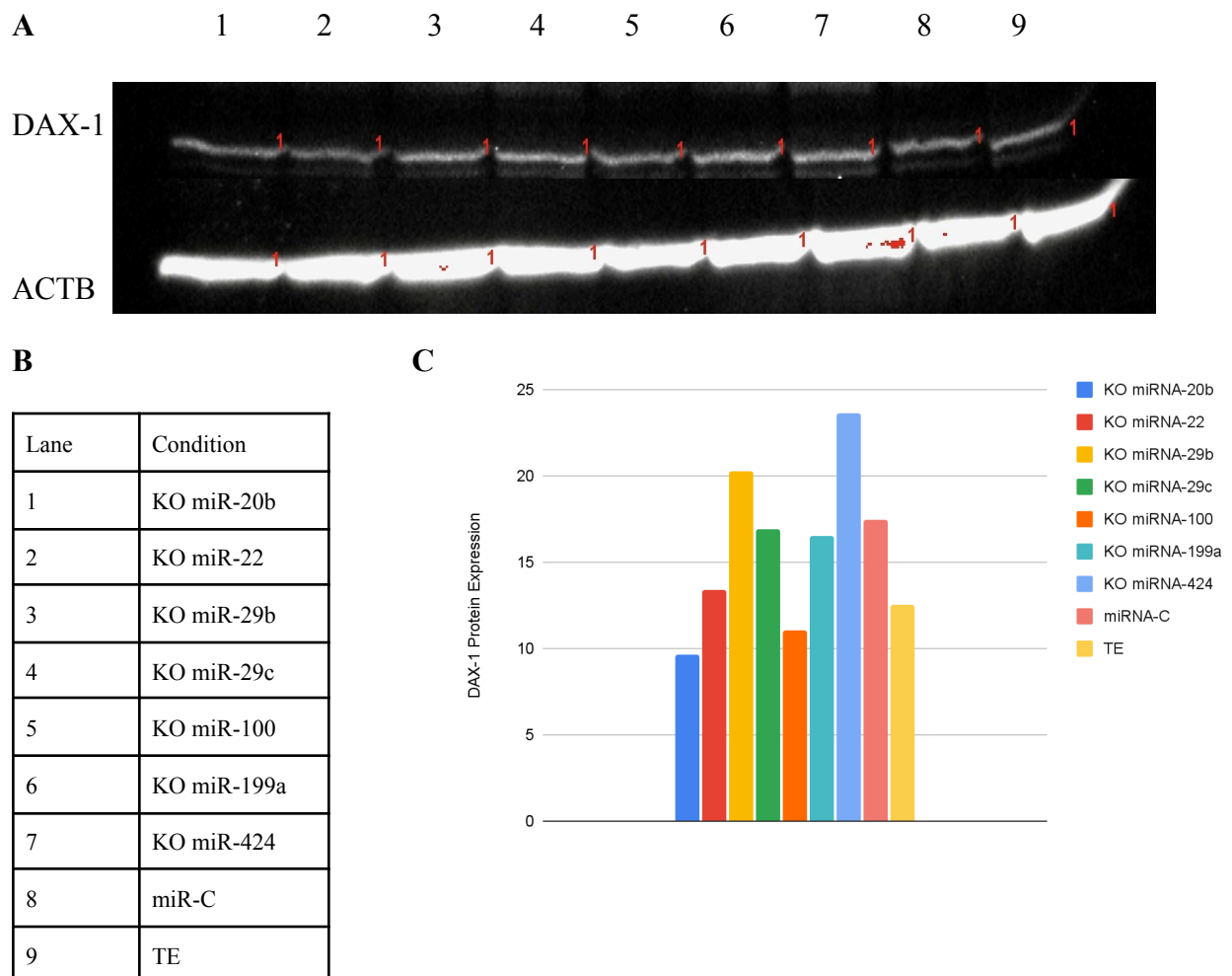


Figure 3-2. DAX-1 Protein Expression in MCF7 Cells after miRNA Inhibitor treatment. A) Western blot image comparing DAX-1 to reference protein beta actin . **B)** key to the western blot data. **C)** western blot quantification via densitometry analysis.

DAX-1 expression following miRNA inhibitor treatment in MCF10A cells

After miRNA inhibitor treatment, RNA isolation, and cDNA synthesis qPCR was performed in order to assess the effect of miRNA inhibition on DAX-1 gene expression in MCF10A cells. As in the previous qPCR experiment, GAPDH was used as the control gene.

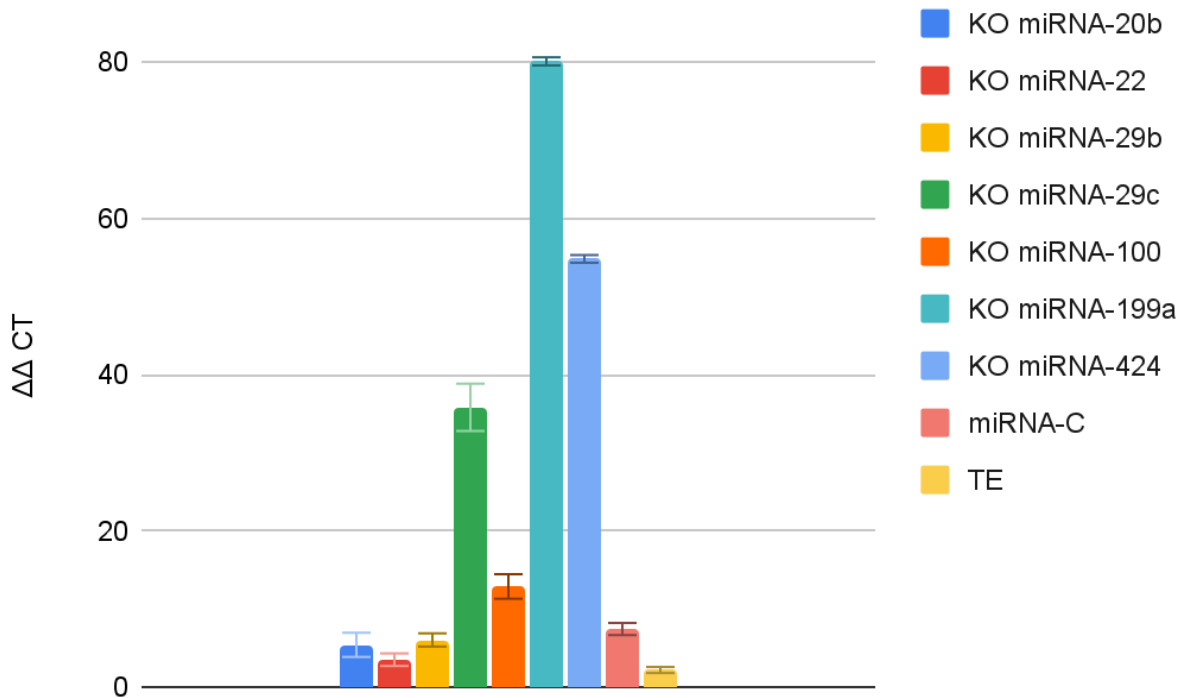


Figure 3-3. DAX-1 mRNA Expression in MCF10A cells after miRNA Inhibitor treatment. qPCR results depicting DAX-1 gene expression levels. Fold changes were calculated by $\Delta\Delta CT$ analysis normalized against GAPDH. Error bars represent standard deviation of the mean.

DAX-1 protein expression following miRNA inhibitor treatment in MCF10A cells

After miRNA inhibitor treatment and protein isolation, western blot analysis was performed in order to assess the effect of miRNA inhibition on DAX-1 protein expression in MCF10A cells.

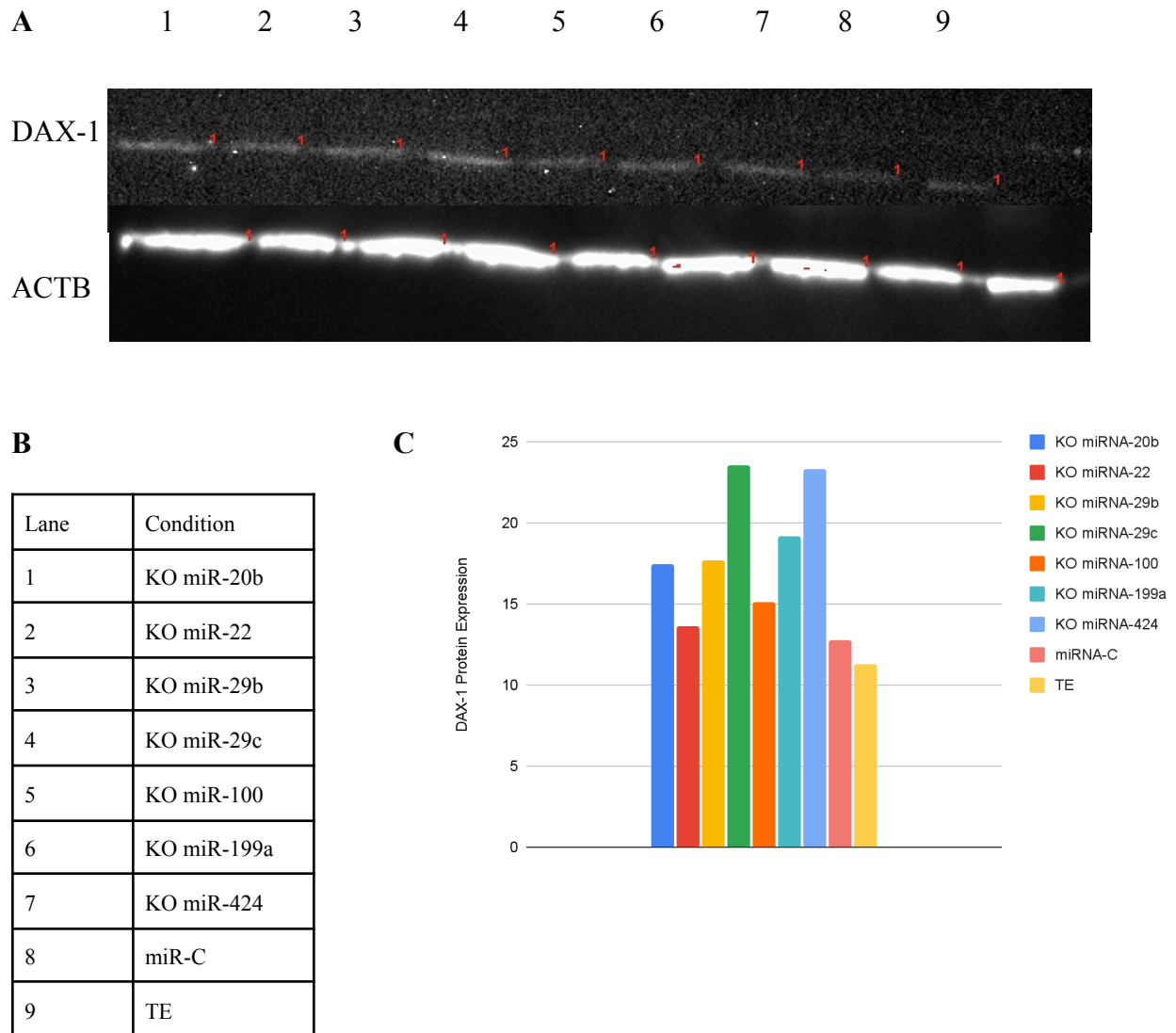


Figure 3-4. DAX-1 Protein Expression in MCF10A Cells after miRNA Inhibitor treatment. A) Western blot image comparing DAX-1 to reference protein beta actin. B) key to the western blot data. C) western blot quantification via densitometry analysis.

DISCUSSION:

Despite overexpression in lung and prostate cancer, DAX-1 downregulation remains one of the many drivers of BC development [18]. Along the same lines, miRNA overexpression has been demonstrated to lead to tumorigenesis in many cancers including BC [29]. Despite extensive research in both of these molecular drivers of BC, only one study examined how miRNAs target DAX-1 leading to its degradation and, ultimately, progression in BC [26]. After inhibiting 7 miRNA that were repeatedly upregulated in BC (Table 2-4), DAX-1 gene and protein expression were analyzed in both MCF7 and MCF10A cells. In MCF7 cells, qPCR results indicated that inhibiting any of the aforementioned miRNA elicited an increase in DAX-1 mRNA expression with the exception of miRNA-29c (Figure 3-1). Additional western blot quantification indicated that inhibiting the 7 specific miRNA led to an increase in DAX-1 expression compared to both controls only in the KO of miR-29b and KO miR-424 (Figure 3-2). This discrepancy in qPCR and WB data is a trend that was observed across experiments, cell lines, and genes of interest.

One possible explanation for this decrease in DAX-1 protein expression not seen in the western blot data could be the action of miRNA family members rescuing the function of specific inhibited relatives. Despite the entire miRNA sequence being capable of binding to its target, published research strongly indicated that the nucleotides located at positions 2-7, known as the “seed” sequence, play a pivotal role in determining target specificity for a miRNA [60 & 61]. Consequently, miRNAs sharing identical seed sequences are anticipated to target closely overlapping gene sets, leading to their classification within the same miRNA family. On the other hand, miRNA clusters are another layer adding to the complexity of miRNA target

identification. Current research predicts at least 30% of miRNAs are situated in polycistronic miRNA clusters whereby multiple miRNA genes are generated from a single primary transcript [62, 63, 64, 65]. Even though the interplay between miRNA families and clusters makes ascertaining specific miRNA targets incredibly challenging, the family groups and cluster relatives can also serve as tools to help infer potential targets of a specific miRNA if it belongs to a certain group. For instance, the miR-17~92 miRNA cluster family consists of 3 closely related and highly conserved polycistronic miRNA genes, which together encode a total of 15 miRNAs. During the early evolution of vertebrates, gene duplication and deletion occurrences led to the emergence of 2 mammalian paralogs: the miRNA-106b~25 cluster and the miRNA-106a~363 cluster [66]. This family is perhaps the most well studied since its disruption leads to issues with vertebrate development and a variety of diseases including cancer [67]. Notably, the same can be said for DAX-1. Since disrupting DAX-1 and the two aforementioned miRNA clusters elicit the same abnormal physiological results there is strong evidence suggesting a relationship exists between this miRNA family and DAX-1. Along the same lines, the data from this chapter as well as previously published results corroborate my main hypothesis that multiple miRNAs negatively regulate DAX-1 expression in BC.

The argument that miRNA-106a targets DAX-1 in BC is supported on the basis of ancestry and the function of the miRNA-17~92 cluster [26]. The results above depict opposite trends when you inhibit miRNA-20b in MCF7 cells and probe for DAX-1 expression in qPCR and WB (Figure 3-1 & Figure 3-2). MiRNA-20b belongs to the miRNA-106b~25 cluster whereas miRNA-20a is a member of the miRNA-17~92 cluster [68]. It is highly probable that miRNA-20a is able to rescue the action of miRNA-20b and subsequently prevent DAX-1 repression in order to “help out” its relatives. This differential miRNA expression among family

and cluster members has been studied extensively, especially in the miRNA-17~92 cluster and its 2 paralog progeny, and has been shown to benefit BC cells [69].

Additionally, 2 of the miRNAs inhibited above are members of the miRNA-29 family (miRNA-29b and 29c). This family are all epigenetic regulators of DNA methylation (epi-miRs) and lead to the development of cancer and its progression by downregulating DNA methyltransferases (DNMTs) [70, 71, 72]. Western blot and qPCR data highlighted that inhibiting miRNA-29b led to an increase in DAX-1 expression however the same trend was not observed when miRNA-29c was inhibited (Figure 3-1 and Figure 3-2). Interestingly, the largest increase in DAX-1 expression in MCF10A cells occurred when miRNA-29c, 199a, and 424 were inhibited for both the western blot and qPCR experiments (Figure 3-4 & 3-5). The data suggests that these 3 miRNA target DAX-1 in MCF10A cells but only miR-199a and miR-424 target DAX-1 in MCF7 cells suggesting that epi-miRs (like the miR-29 family) are likely not a pertinent pathway to downregulate DNMTs since evidence indicates DAX-1 is downregulated via methylation in BC [73].

Finally, inhibiting miRNA-100 correlates to an increase in DAX-1 mRNA levels and protein expression (Figure 3-1 & Figure 3-2). Similar to the other miRNAs that are inhibited which are described in this chapter, miRNA-100 and its relatives seem to have a dual role as either a tumor suppressor or promoter depending on the cancer, hormone expression, and tissue profile [74]. To conclude, western blot and qPCR analysis highlighted 4 miRNA that could potentially target DAX-1 in MCF7 cells. These miRNA are: miRNA-29b, 100, 199a and 424. In summation, the identification of these 4 additional miRNAs offer new insight into the complexity of miRNA targeting as well as BC potentiation.

CHAPTER 4:

EFFECT OF miRNA INHIBITION ON ER α AND CCND1 EXPRESSION

INTRODUCTION:

Estrogen Receptor α (ER α) is a nuclear hormone receptor (NHR), encoded by the *ESR1* gene, that mediates the effects of estradiol (E2) in various tissues, including the breast, uterus, brain, heart, and bone. In breast tissue, ER α functions primarily as a transcription factor [75]. Similar to other NHRs, when E2 binds to ER α , the receptor undergoes conformational changes, leading to its dimerization and translocation into the nucleus. As a transcription factor, ER α directly binds to specific DNA sequences known as estrogen response elements (EREs) within the regulatory regions of target genes, modulating a cellular response [76]. The activation of ER α signaling is critical for normal mammary gland development and function, as well as for the growth and maintenance of hormone-sensitive BC cells. Approximately 70-80% of BC express ER α including MCF7 cells [76]. In MCF7 cells, E2 signaling through ER α promotes tumor growth and progression which correlates with DAX-1 underexpression. Previous research in the Tzagarakis-Foster lab investigated the effects of DAX-1 transfection in MCF7 cells in order to better understand this pathway. When DAX-1 was added to ER α positive MCF7 cells, cell proliferation and estradiol activation of the cyclin D1 gene (*CCND1*) were blocked [18]. Ergo, DAX-1 has been identified as a corepressor of ER α [18 & 77]. Ultimately, I designed my experiments to not only understand the effects of miRNA inhibition on ER α , which is downstream of DAX-1, but also elucidate the effects of miRNA inhibition on a key downstream target of ER α : *CCND1*.

CCND1 is a regulatory protein that is responsible for cell growth and proliferation. It is encoded by the *CCND1* gene and functions as a regulatory subunit of cyclin-dependent kinase (CDK) complexes. *CCND1* binds to CDK4, forming active cyclin-CDK complexes that phosphorylate and subsequently inactivate the retinoblastoma protein (pRb) [78]. This

phosphorylation-inactivation mechanism of pRb activates E2F, a transcription factor, to transcribe genes necessary for the cell to progress from G1 to S phase, the period of DNA replication during the cell cycle [78]. Abnormal *CCND1* expression is commonly observed in various cancers, including breast cancer [78]. Overexpression of CCND1 can promote uncontrolled cell proliferation and tumor growth by driving aberrant cell cycle progression [78]. In BC, CCND1 is frequently overexpressed in hormone receptor-positive (HR+) subtypes such as MCF7 cells. Besides the canonical function of CCND1, this overexpression in BC is also a result of independent CCND1 activity. Without a CDK4, CCND1 can bind to NHRs such as peroxisome proliferator-activated receptor gamma (PPAR γ), androgen receptor (AR), and ER α as another mechanism to potentiate uncontrolled cell growth and proliferation [79]. By comparing the extent of miRNA targeting of ER α and CCND1 in MCF7 and MCF10A cells, these data offer a broader understanding of how miRNA contributes to the DAX-1/ER α /CCND1-axis in HR+ BC compared to normal breast epithelial cells.

METHODS:*Cell Culture*

All cells used in these experiments were stored in an incubator set to 37°C and 5% carbon dioxide. The cells were passaged every three days with MCF7 and MCF10A cells in DMEM and MEGM SingleQuots™ Supplement Pack (Lonza, Basel, Switzerland) media respectively. The media was purchased from Thermo Fisher. DMEM was sustained with 50 milliliters of FBS and 5% PenStrep. MCF10A received 50 milliliters of FBS and additional media supplements (Lonza, Basel, Switzerland).

miRNA inhibitor

Once the MCF7 and MCF10a cells reach confluency, miRCURY LNA™ miRNA Power Inhibitors (Qiagen, Venlo, Netherlands) were used in order to knockdown the specific miRNA. The protocol was followed closely and cell lysate was collected following a 72 hour incubation. The inhibitors were consistently added at a concentration of 500 nM and TE buffer was used for the vehicle control.

Table 4-1. miRCURY LNA™ miRNA Power Inhibitors

miRNA inhibitors	Sequence (5' → 3')	Company
hsa-miR-20b-5p	ACCTGCACTATGAGCACTTT	QIAGEN, Venlo, Netherlands
hsa-miR-22-3p	CAGTTCTTCAACTGGCAGCT	QIAGEN, Venlo, Netherlands
hsa-miR-29b-3p	ACTGATTTCAAATGGTGCT	QIAGEN, Venlo, Netherlands
hsa-miR-29c-3p	CCGATTTCAAATGGTGCT	QIAGEN, Venlo, Netherlands
hsa-miR-100-5p	ACAAGTTCGGATCTACGGGT	QIAGEN, Venlo, Netherlands
hsa-miR-199a-3p	AACCAATGTGCAGACTACTG	QIAGEN, Venlo, Netherlands
hsa-miR-424-5p	AAACATGAATTGCTGCT	QIAGEN, Venlo, Netherlands
Negative Control A	TAACACGTCTATACGCCCA	QIAGEN, Venlo, Netherlands

Reverse Transcription

The qScript™ cDNA SuperMix kit (Quantabio, Beverly, MA) was used to synthesize cDNA from the isolated RNA. The concentration for all cDNA synthesis was 400nM and the directions were completed according to the manufacturer's instructions.

Quantitative PCR

cDNA synthesis from extracted mRNA was used as a template for qPCR. qPCR reactions were performed in triplicate using the BioRad CFX96 Real-Time PCR system (BioRad, Hercules, CA) qPCR reactions were prepared using 10µL of SYBR Green Master Mix (Life Technologies, Carlsbad, CA) or QuantiTect SYBR Green PCR kit (Qiagen, Venlo, Netherlands), 0.5µL of 10µM forward and reverse primers, 7.5µL of dH₂O, and 2µL of cDNA. GAPDH housekeeping gene was used as control and experimental genes were compared to GAPDH as a baseline. The $\Delta\Delta CT$ method was used to calculate gene expression and the error bars on qPCR results represent standard deviation of the mean.

Table 4-2. List of Primers used for qPCR

Primer	Forward Sequence (5' → 3')	Reverse Sequence (5' → 3')
ER α	GACAGGGAGCTGGTTCACAT	AGGATCTCTAGCCAGGCACA
CCND1	GCATGTTCGTGGCCTCTAAG	CGTGTTTGCGGATGATCTGT

Table 4-3. List of Annealing Temperatures for qPCR

Primer	Annealing Temperature qPCR
ER α	59°C
CCND1	59°C
GAPDH	59°C

Table 4-4. Thermal Cycler Conditions for two-step Amplification qPCR

Step	Temperature	Time
Initial Denaturation	95°C	2 minutes
50 Cycles:		
Denaturation	95°C	15 seconds
Annealing	59°C	1 minute
+Plate Read		
Hold	4°C	∞

Protein Isolation and Quantification

For protein isolation, cells were washed twice in ice cold 1X PBS and lysed in RIPA lysis buffer (25 mM Tris•HCl pH 7.6, 150 mM NaCl, 1% NP-40, 1% sodium deoxycholate, 0.1% SDS) including Halt Protease Inhibitors (Thermo Fisher, Waltham, MA) for 15 minutes at 4°C. Following cell lysis, the lysate was sonicated or passed through a syringe with a 21-gauge needle 4-5 times to breakdown genomic DNA and facilitate protein isolation. Sonicated lysates were centrifuged at 14,000 rpm, for 15 minutes at 4°C and the supernatant was transferred to a new microcentrifuge tube. After isolation, the protein samples were quantified using a BCA assay and stored in a -80°C freezer.

Western Blot

Equivalent amounts of various cell lysates were prepared including LDS Sample Buffer and 10X reducing agent (Thermo Fisher, Waltham, MA) that was compatible with the NuPAGE electrophoresis system. Samples were electrophoresed through a 10% SDS-PAGE gel and wet transferred for 1 hour to a PVDF membrane for blotting. Blots were washed with DI water twice, before a 10 minute incubation at room temperature in the SuperSignal™ Western Blot Enhancer Antigen Pretreatment Solution (Thermo Fisher, Waltham, MA), 5 DI water washes were performed before blots were blocked for 60 minutes at room temperature with 10% Bovine Serum Albumin in 1X Tris-buffered Saline (TBS) with 0.1% Tween (1X TTBS). Following blocking, and 1X TTBS washes, primary antibody was added to each blot in the SuperSignal™ Western Blot Enhancer Primary Antibody (Thermo Scientific, Waltham, MA) Diluent and incubated overnight at 4°C with rocking. The following day, blots were washed with 1X TTBS and incubated with either anti-rabbit or anti-mouse secondary antibody (diluted 1:2000 in blocking solution) for 60 minutes at room temperature with rocking. Blots were washed with 1X TTBS and chemiluminescent (Azure Biosystems, Dublin, CA) detection of proteins will be performed using the GelDoc Imaging System (BioRad, Hercules, CA).

Table 4-5. List of Antibodies used for Western Blotting

Protein	Species	Company	Dilution Factor
ER α	Rabbit (Polyclonal)	Thermo Fisher Scientific, Waltham, MA	1:500
CCND1	Rabbit (Polyclonal)	Invitrogen, Carlsbad, CA	1:500
ACTB	Mouse (Monoclonal)	Thermo Fisher Scientific, Waltham, MA	1:1000

RESULTS:

ER α gene expression following miRNA inhibitor treatment in MCF7 cells

After miRNA inhibitor treatment, RNA isolation, and cDNA synthesis qPCR was performed in order to assess the effect of miRNA inhibition on ER α gene expression in MCF7 cells.

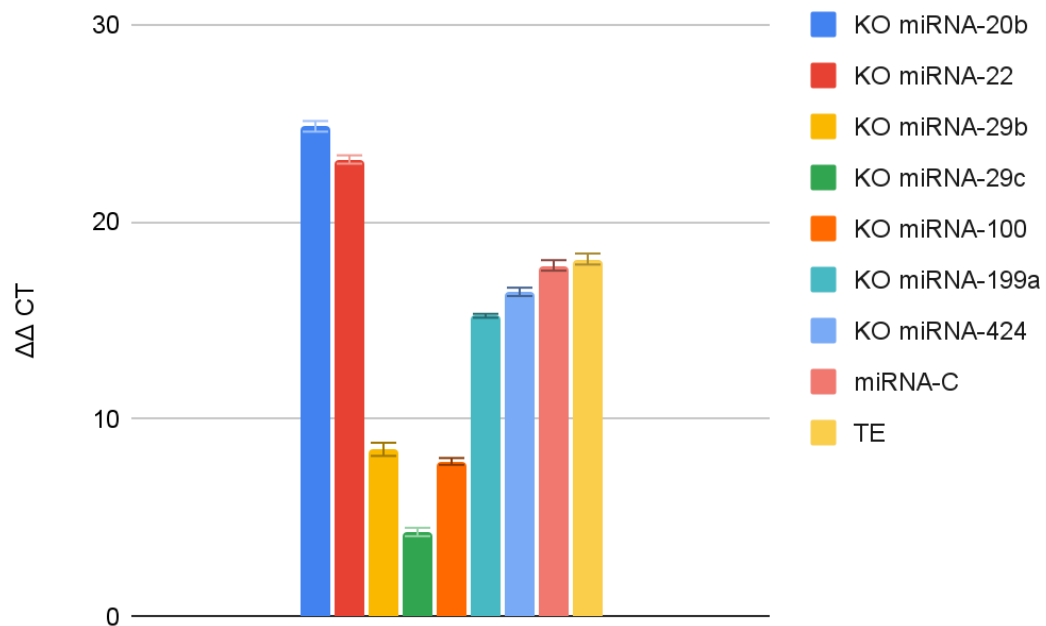


Figure 4-1. ER α mRNA Expression in MCF7 Cells after miRNA Inhibitor Treatment. qPCR results depicting ER α gene expression levels. Fold changes were calculated by $\Delta\Delta CT$ analysis normalized against GAPDH. Error bars represent standard deviation of the mean.

ER α protein expression following miRNA inhibitor treatment in MCF7 cells

After miRNA inhibitor treatment and protein isolation, a western blot was performed in order to assess the effect of miRNA inhibition on ER α protein expression in MCF7 cells.

Interestingly, ER α protein expression was increased compared to both controls across all of the miRNA inhibition treatments.

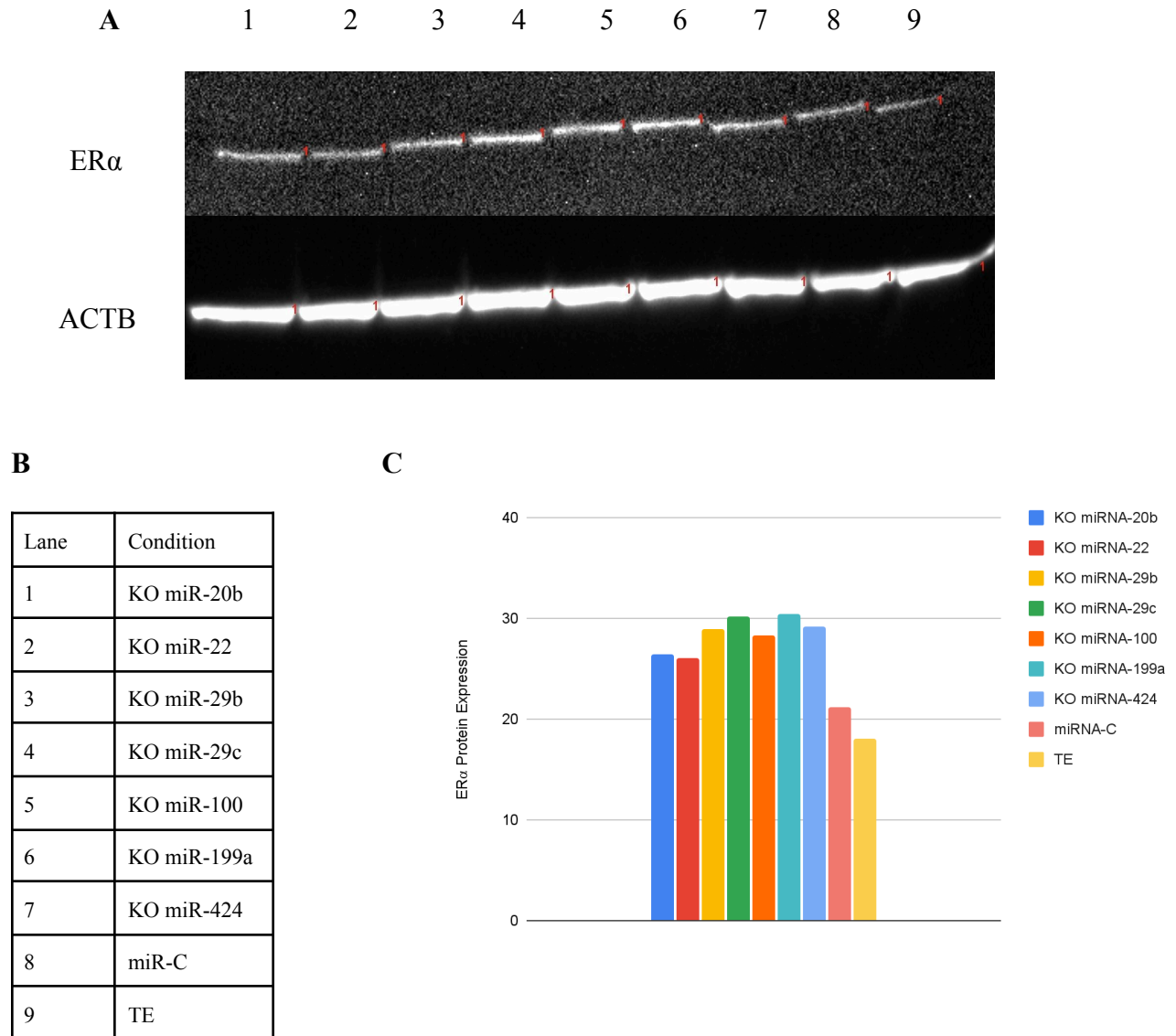


Figure 4-2. ER α Protein Expression in MCF7 Cells after miRNA Inhibitor Treatment. A) WB image comparing DAX-1 to reference protein beta actin . **B)** key to the western blot data. **C)** western blot quantification via densitometry analysis.

ER α gene expression following miRNA inhibitor treatment in MCF10A cells

After miRNA inhibitor treatment, RNA isolation, and cDNA synthesis qPCR was performed in order to assess the effect of miRNA inhibition on ER α gene expression in MCF10A cells.

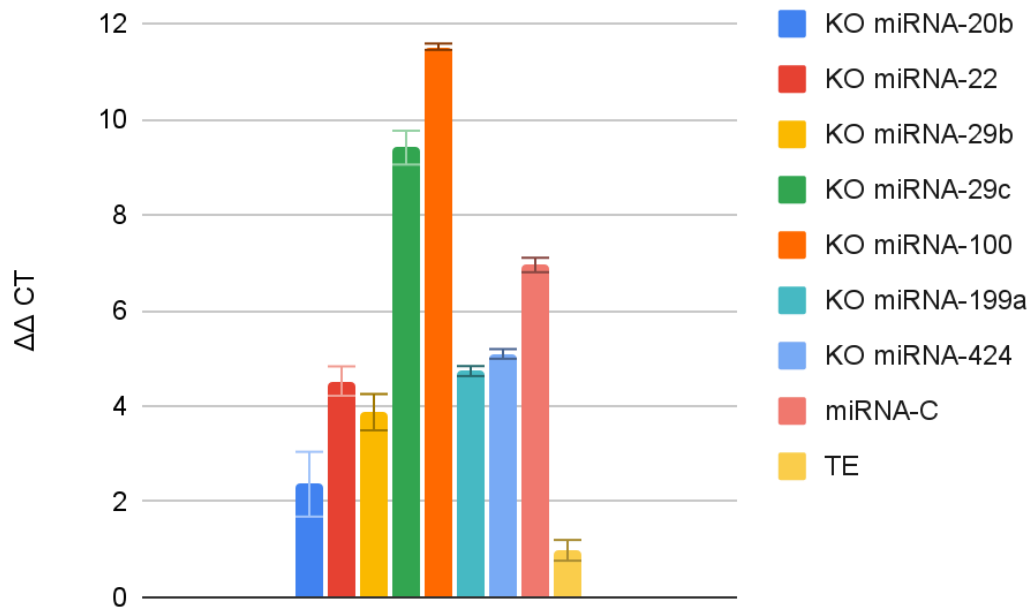
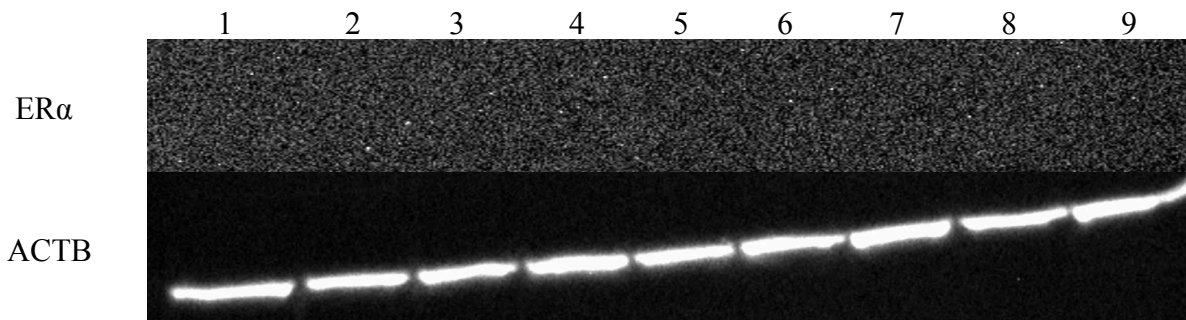


Figure 4-3. ER α mRNA Expression in MCF10A Cells after miRNA Inhibitor Treatment. qPCR results depicting ER α gene expression levels. Fold changes were calculated by $\Delta\Delta CT$ analysis normalized against GAPDH. Error bars represent standard deviation of the mean.

ER α protein expression following miRNA inhibitor treatment in MCF10A cells

After miRNA inhibitor treatment and protein isolation, a western blot was performed in order to assess the effect of miRNA inhibition on ER α protein expression in MCF10A cells. Beta actin was used as the reference protein.

A



B

Lane	Condition
1	KO miR-20b
2	KO miR-22
3	KO miR-29b
4	KO miR-29c
5	KO miR-100
6	KO miR-199a
7	KO miR-424
8	miR-C
9	TE

Figure 4-4. ER α Protein Expression in MCF10A Cells after miRNA Inhibitor Treatment.

A) Consistent with previous data in the Tzagarakis-Foster lab, ER α was undetectable by western blot in MCF10A cells. **B)** key to the western blot data.

CCND1 gene expression following miRNA inhibitor treatment in MCF7 cells

After miRNA inhibitor treatment, RNA isolation, and cDNA synthesis, qPCR was performed in order to assess the effect of miRNA inhibition on *CCND1* gene expression in MCF7 cells. As shown in Figure 4-5, inhibition of miRNA-29c results in the greatest expression of the *CCND1* gene, in fact, greater than control levels of expression.

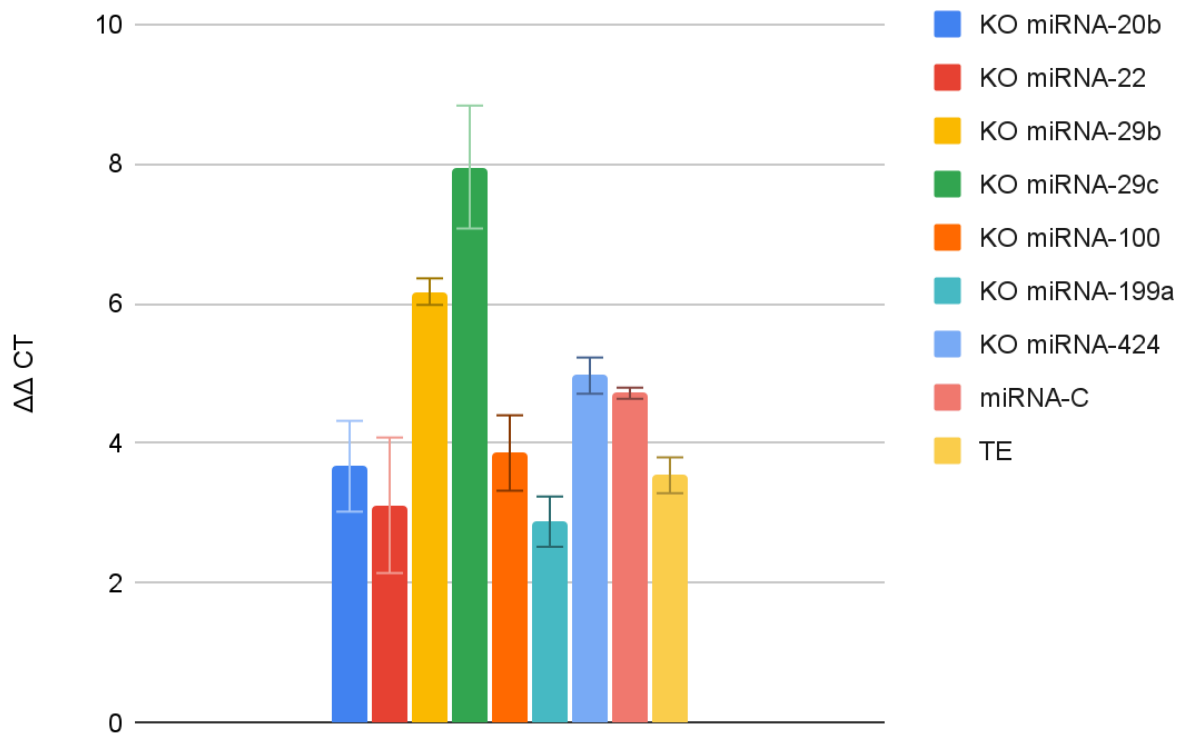


Figure 4-5. *CCND1* mRNA Expression in MCF7 Cells after miRNA Inhibitor Treatment. qPCR results depicting *CCND1* gene expression levels. Fold changes were calculated by $\Delta\Delta CT$ analysis normalized against GAPDH. Error bars represent standard deviation of the mean.

CCND1 protein expression following miRNA inhibitor treatment in MCF7 cells

After miRNA inhibitor treatment and protein isolation, a western blot was performed in order to assess the effect of miRNA inhibition on CCND1 protein expression in MCF7 cells.

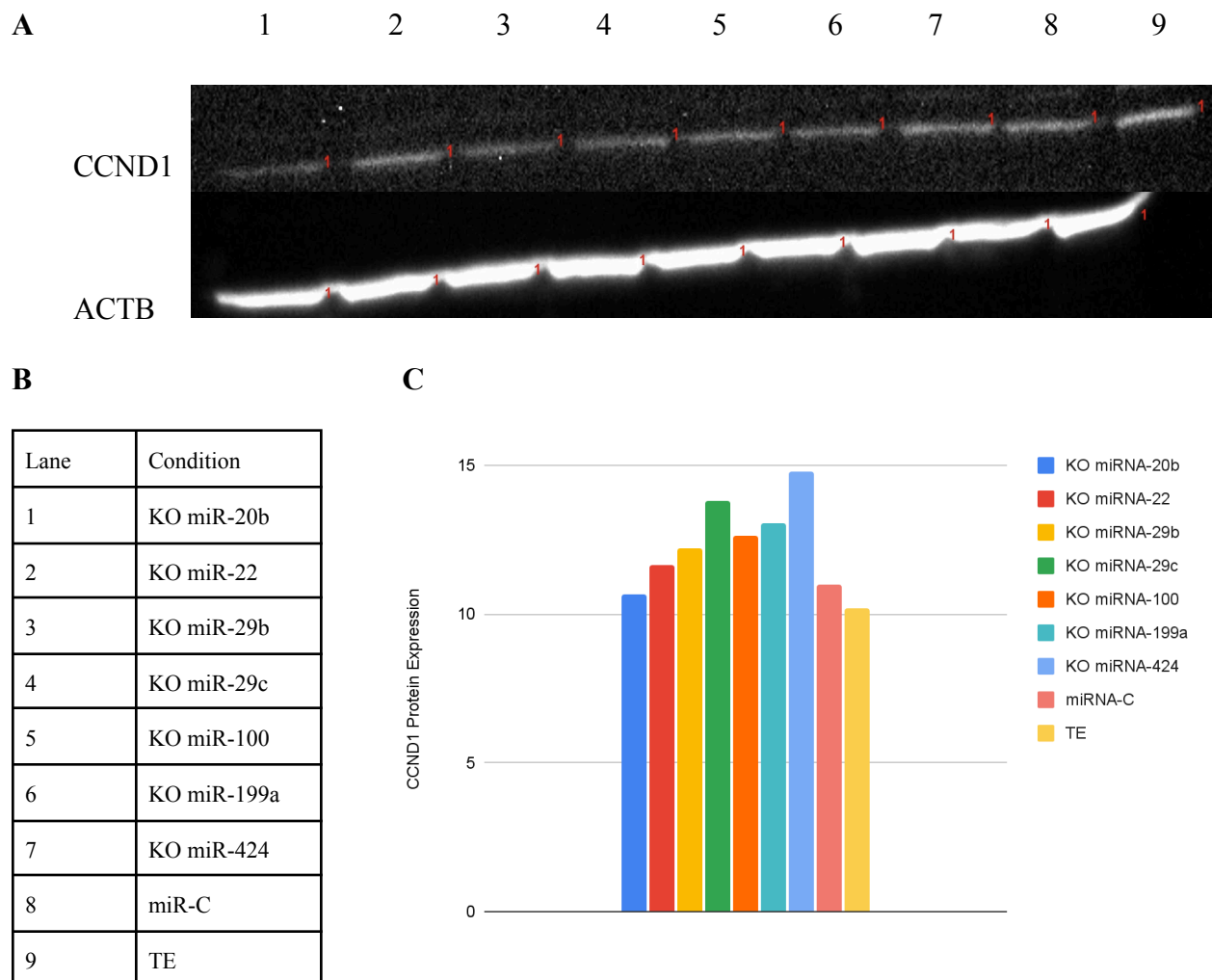


Figure 4-6. CCND1 Protein Expression in MCF7 Cells after miRNA Inhibitor Treatment.

A) Western blot image comparing DAX-1 to reference protein beta actin. **B)** key to the western blot data. **C)** western blot quantification via densitometry analysis.

CCND1 gene expression following miRNA inhibitor treatment in MCF710A cells

After miRNA inhibitor treatment, RNA isolation, and cDNA synthesis, qPCR was performed in order to assess the effect of miRNA inhibition on *CCND1* gene expression in MCF10A cells. Interestingly, due to the replicative immortality necessary for MCF10A cells to be grown in culture, there was an increase in *CCND1* gene expression compared to the MCF7 cells.

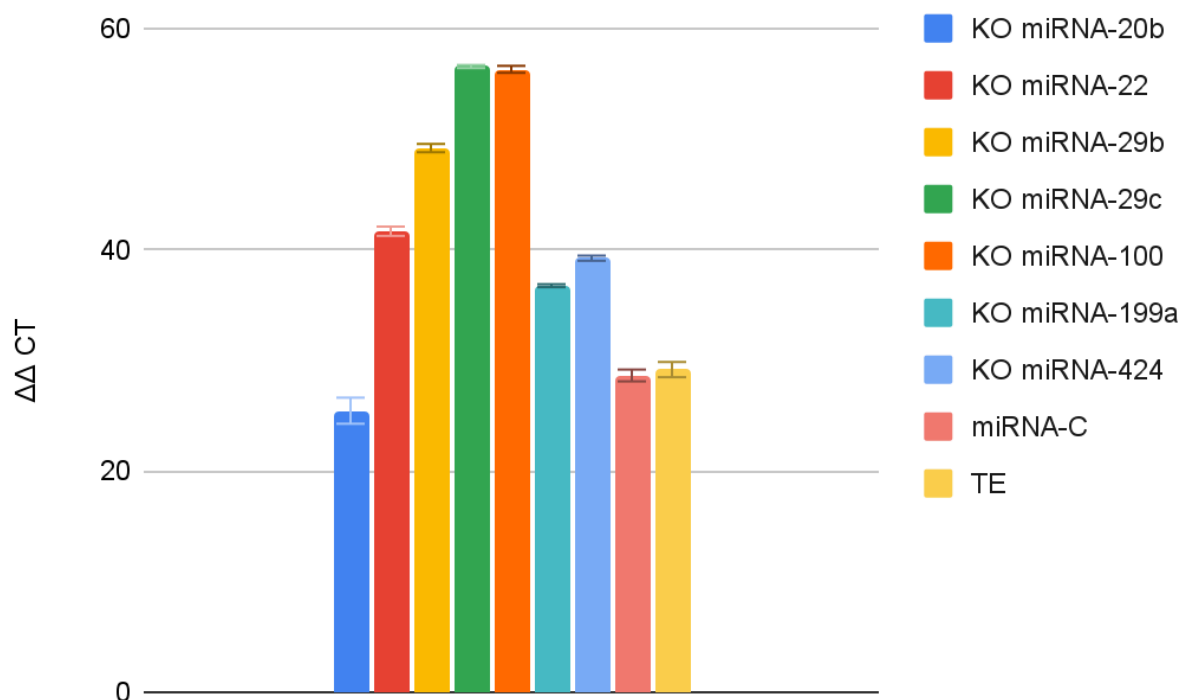


Figure 4-7. CCND1 mRNA Expression in MCF10A Cells after miRNA Inhibitor Treatment. qPCR results depicting *CCND1* gene expression levels. Fold changes were calculated by $\Delta\Delta CT$ analysis normalized against GAPDH. Error bars represent standard deviation of the mean.

CCND1 protein expression following miRNA inhibitor treatment in MCF10A cells

After miRNA inhibitor treatment and protein isolation, western blot analysis was performed in order to assess the effect of miRNA inhibition on CCND1 protein expression in MCF10A cells. The seemingly contradictory data in this chapter was not expected. However, miRNA and oncology research have suggested that miRNAs target the cell cycle pathway via CCND1 (80). The research in this chapter corroborates published literature once again highlighting the intricacy of miRNA dysregulation. Cancers upregulate hundreds of miRNA in order for some cellular physiological benefit, the downside, but beneficial clinically, is that some of these miRNA target advantageous proteins and pathways such as CCND1.

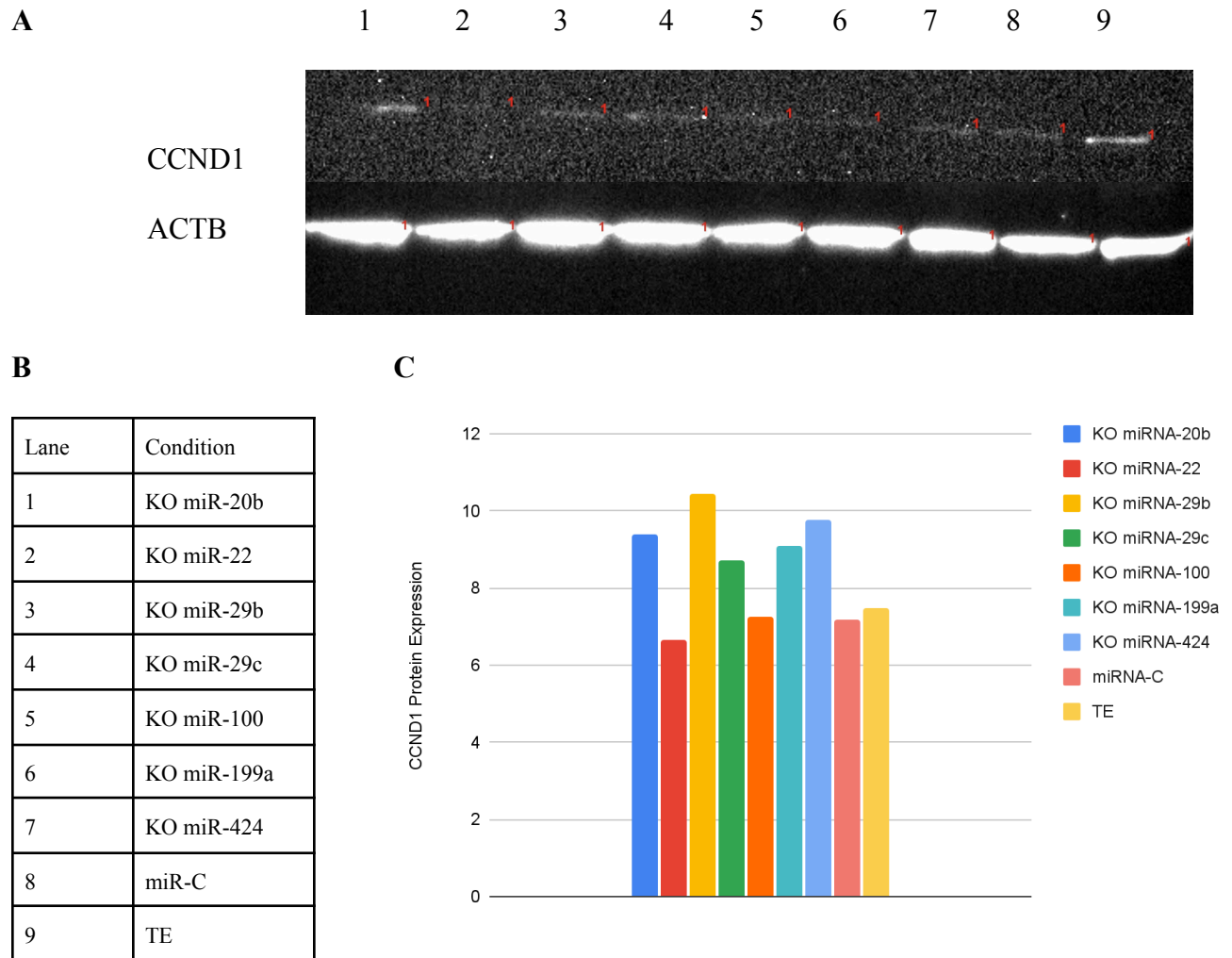


Figure 4-8. CCND1 Protein Expression in MCF10A Cells after miRNA Inhibitor Treatment. **A)** Western blot image comparing DAX-1 to reference protein beta actin. **B)** key to the western blot data. **C)** western blot quantification via densitometry analysis.

DISCUSSION:

Overexpression of ER α and CCND1 has been noted as a key driver of uncontrolled growth and proliferation in HR+ BC such as MCF7 cells [81]. After inhibiting 7 miRNA that were repeatedly upregulated in BC (Table 2-4), ER α and CCND1 gene and protein expression were analyzed in both MCF7 and MCF10A cells to examine the extent of miRNA-driven downregulation.

ER α Analysis

In MCF7 cells, qPCR data indicated that only inhibiting miR-20b and miR-22 led to an increase in ER α gene expression compared to the controls (Figure 4-1). In fact, KO the other 5 miRNAs led to a decrease in ER α expression (Figure 4-1). Conversely, WB results portray that inhibiting any of the 7 miRNA elicited an increase in ER α protein expression compared to both controls (Figure 4-2). The first inference made from this data remains that miR-20b and miR-22 both downregulate ER α . This result corroborates other published literature in the field describing miR-20b and 22 as drivers of BC growth through different pathways despite targeting ER α [82, 83, 84, 85]. For instance, research has demonstrated miR-20b targets phosphatase and tensin homologue (PTEN) [86]. By targeting and subsequently downregulating PTEN, a potent tumor suppressor gene, miR-20b directly contributes to MCF7 cell proliferation [86]. Interestingly, miR-20b and miR-22 possess extremely different lineages. MiR-20b is a member of the master regulator miR-17~92 family, whereas miR-22 belongs to no family group or cluster [66 & 87]. Since ER α is so paramount for HR+ BC to survive, it is probable that the western blot results are a result of additional miRNAs rescuing the inhibition of ER α at the transcriptional level and increasing its translation [88]. Additionally, previous data from this thesis research (Chapter 3) indicates that miR-29b, 100, 199a, and 424 downregulate DAX-1. Since DAX-1 represses ER α

transcription, it is likely that inhibiting these 4 miRNA led to the overexpression of ER α since these miRNA are inhibiting an inhibitor of ER α .

In MCF10A cells, there seemed to be an off-target effect of the miR-C inhibitor which increased ER α expression compared to the much more physiologically accurate TE buffer vehicle control (Figure 4-3). Similar to the MCF7 cells, there was an increase in ER α expression across all inhibited miRNA especially miR-29c and miR-100 in the MCF10A cells (Figure 4-3). In both the MCF7 and MCF10A cells, unexpected upregulation of ER α could be the result of activated forkhead box protein A1 (FOXA1). FOXA1 is a hepatocyte nuclear factor upstream of ER α [88]. FOXA1 as a “pioneer factor” enhances the binding of ER to the ERE leading to an increased effect of ER α function [89 & 90]. Pioneering factors are essentially “stronger” transcription factors with the ability to bind to more condensed chromatin and ultimately increase gene expression. As a transcription factor, FOXA1 has been shown to not only be overexpressed in BC, driving ER α -dependent proliferation but also can modulate ER binding in non BC cells [90 & 91]. In addition, several miRNA, including miRNA-100, are known to target FOXA1 in BC leading to its downregulation [92]. Overall, multiple pathways, in addition to those explored in this chapter, could be responsible for the increased ER α expression observed in the MCF7 and MCF10A cells.

CCND1 Analysis

Additional analysis was conducted to ascertain the effect of miRNA inhibition on CCND1 expression. In MCF7 cells, qPCR and western blot results illustrated that inhibiting miR-29b, 29c, and 424 (a member of the miR-16 family) increased CCND1 expression compared to both controls (Figure 4-5 & Figure 4-6). The miRNA-29 and miRNA-16 families have both been identified as regulators of the cell cycle with their ability to target CCND1 [93, 94, 95]. While the downregulation of CCND1 seems to be paradoxical to BC progression, miR-29b, 29c and 424 are all able to potentiate BC through different mechanisms. For instance, evidence strongly suggests miR-29b downregulates complement C1q tumor necrosis factor-related protein 1 (C1QTNF1), secreted protein acidic and rich in cysteine (SPARC), and collagen alpha-2(IV) chain (COL4A2) [96]. Furthermore, downregulation of either C1QTNF1, SPARC, or COL4A2 was sufficient in improving the invasive capabilities of MCF7 cells [96]. While miR-29c is typically downregulated in BC, its upregulation and subsequent inhibition of CCND1 has been shown to promote migration of BC cells and is linked to poor prognostics in BC patients [97]. Along the same lines, miR-424, despite downregulating CCND1 and limiting uncontrolled growth, also targets programmed cell death protein 4 (PCDC4) [98]. By inhibiting PCDC4, miR-424 contributes to the anti-apoptotic capabilities of BC. In MCF10A cells, CCND1 expression was broadly upregulated when all 7 miRNAs were inhibited (Figure 4-7 & Figure 4-8). In summation, as a driver of aberrant growth, CCND1 overexpression is a tenet of BC development. However, the same miRNA responsible for CCND1 downregulation (miR-29b, 29c, and 424) contribute to BC potentiation via invasive and anti-apoptotic cascades.

CHAPTER 5:
EFFECT OF miRNA INHIBITION ON THE MIGRATORY CAPABILITIES
OF MCF7 CELLS

INTRODUCTION:

Sustained proliferative signaling and migration are two key members of the seven hallmarks of cancer. As mentioned in Chapter 4, Cyclin D1 (CCND1), a downstream target of ER α , is one of the many proteins involved in breast cancer (BC) cells' ability to proliferate rapidly. Additional pathways contribute to BC's ability to migrate or invade eventually leading to epithelial-mesenchymal transition (EMT). This process is crucial in development and wound healing, but is overrun and is the canonical method for tumor metastasis [99]. In breast cancer, this process always begins with the primary tumor invading the basement membrane, entering blood vessels or lymph nodes, and finally establishing secondary tumors in distant organs [100]. The scratch-and-heal assay has been used extensively to compare the migratory abilities of cancer cells which are necessary for EMT [101, 102, 103]. Cells are plated in a monolayer and a horizontal scratch is made in order to assess the ability of the cancer cells to fill the wound. This is a standard method of measuring migration in cancer cells. While additional assays could have been performed such as tubal formation to measure angiogenesis, or creating a double layer of cancer cells on top of non-malignant cells and assessing invasion, the purpose of this chapter remains to analyze the effect of miRNA inhibition on the migratory and proliferative abilities of MCF7 cells via scratch-and-heal assays.

METHODS:

Cell Culture

All cells used in these experiments were stored in an incubator set to 37°C and 5% carbon dioxide. The cells were passaged every three days with MCF7 and MCF10A cells in DMEM and MEGM SingleQuots™ Supplement Pack (Lonza, Basel, Switzerland) media respectively. The media was purchased from Thermo Fisher. DMEM was sustained with 50 milliliters of FBS and 5% PenStrep. MCF10A received 50 milliliters of FBS and additional media supplements (Lonza, Basel, Switzerland).

miRNA inhibitor

Once the MCF7 and MCF10a cells reach confluency, miRCURY LNA™ miRNA Power Inhibitors (Qiagen, Venlo, Netherlands) were used in order to knockdown the specific miRNA. The protocol was followed closely and cell lysate was collected following a 72 hour incubation. The inhibitors were consistently added at a concentration of 500 nM and TE buffer was used for the vehicle control.

Table 5-1. miRCURY LNA™ miRNA Power Inhibitors

miRNA inhibitors	Sequence (5' → 3')	Company
hsa-miR-29c-3p	CCGATTTCAAATGGTGCT	QIAGEN, Venlo, Netherlands
hsa-miR-199a-3p	AACCAATGTGCAGACTACTG	QIAGEN, Venlo, Netherlands
hsa-miR-424-5p	AAACATGAATTGCTGCT	QIAGEN, Venlo, Netherlands
Negative Control A	TAACACGTCTATACGCCCA	QIAGEN, Venlo, Netherlands

Scratch-and-heal Assay

MCF7 cells were seeded on a 96-well plate at a concentration of 20,000 cells per well. After the cells reached 100% confluency (approximately after 48-72 hours) the WoundMaker™ (Essen BioScience) was used to create a horizontal scratch in each well. After 2 washes with 1X PBS, specific miRNA inhibitors at a concentration of 500nM were added to each of the wells and the plate was placed in the IncuCyte™. After initial calibration, repeat scanning was scheduled every (2-3) hours for 72 hours.

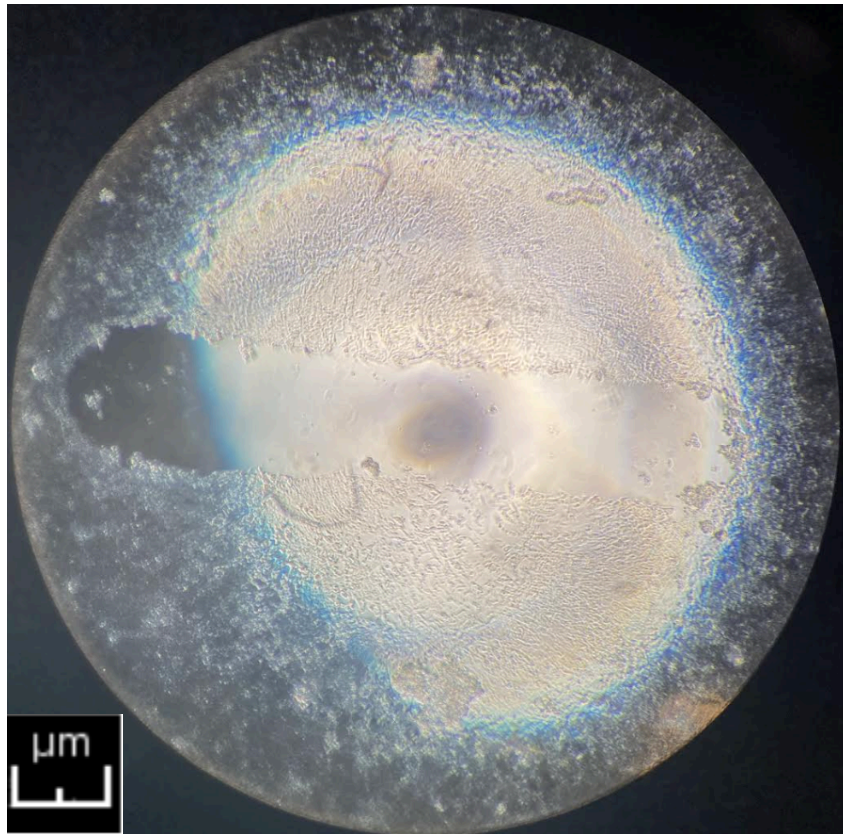


Figure 5-1. Sample Scratch of MCF7 cells. A microscopy image (10X) depicting MCF7 cells 100% confluent. A horizontal scratch is visible due to the WoundMaker™.

	1	2	3	4	5
A					
B	KO MiRNA 29c 500 ng/ml MCF7 (1) 20K / well	KO MiRNA 199a 500 ng/ml MCF7 (1) 20K / well	KO MiRNA 424 500 ng/ml MCF7 (1) 20K / well	MiRNA control 500 ng/ml MCF7 (1) 20K / well	TE 500 ng/ml MCF7 (1) 20K / well
C					

Figure 5-2. IncuCyte Plate Map. 15 wells were used in total. The 5 treatment conditions were: KO-miR-29c, KO-miR-199a, KO-miR-424, miR-C and TE buffer as the vehicle control. Each condition was performed in triplicate.

RESULTS:

72 hour microscopy analysis following miRNA-29c inhibition in MCF7 cells

After miR-29c inhibitor treatment, a scratch-and-heal assay was performed in order to assess the effect of miRNA inhibition on the migratory capabilities of MCF7 cells.

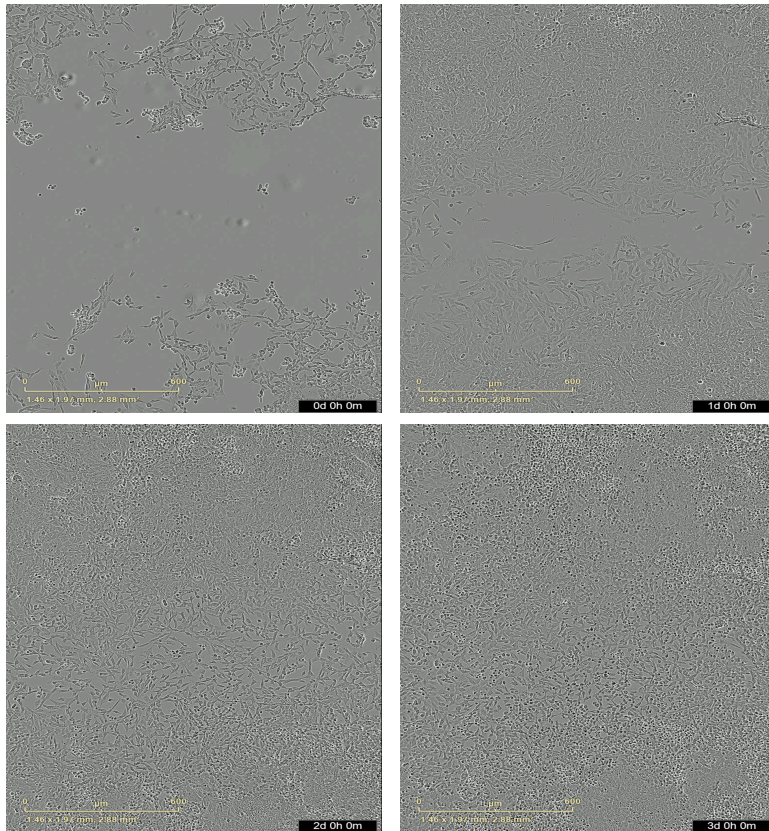


Figure 5-3. Scratch-and-heal Microscopy with KO miR-29c in MCF7 cells. All treatment conditions were plated in triplicate. Images were taken every 12 hours for 3 days. The images above are a representative sample of the dozens of images acquired.

72 hour microscopy analysis following miRNA-199a inhibition in MCF7 cells

After miR-199a inhibitor treatment, a scratch-and-heal assay was performed in order to assess the effect of miRNA inhibition on the migratory capabilities of MCF7 cells.

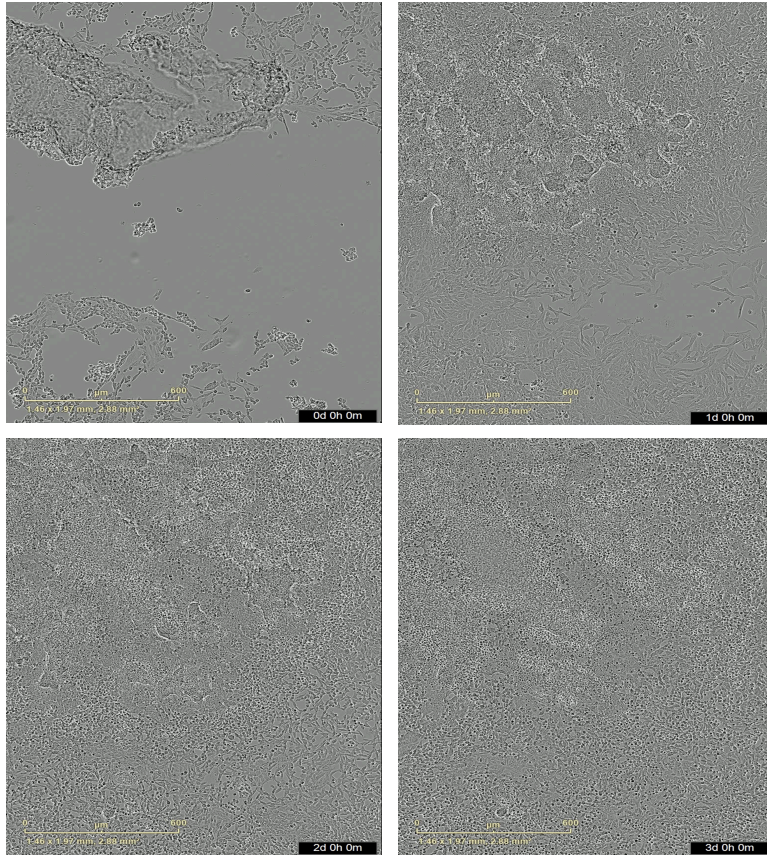


Figure 5-4. Scratch-and-heal Microscopy with KO miR-199a in MCF7 cells. All treatment conditions were plated in triplicate. Images were taken every 12 hours for 3 days. The images above are a representative sample of the dozens of images acquired.

72 hour microscopy analysis following miRNA-424 inhibition in MCF7 cells

After miR-424 inhibitor treatment, a scratch-and-heal assay was performed in order to assess the effect of miRNA inhibition on the migratory capabilities of MCF7 cells.

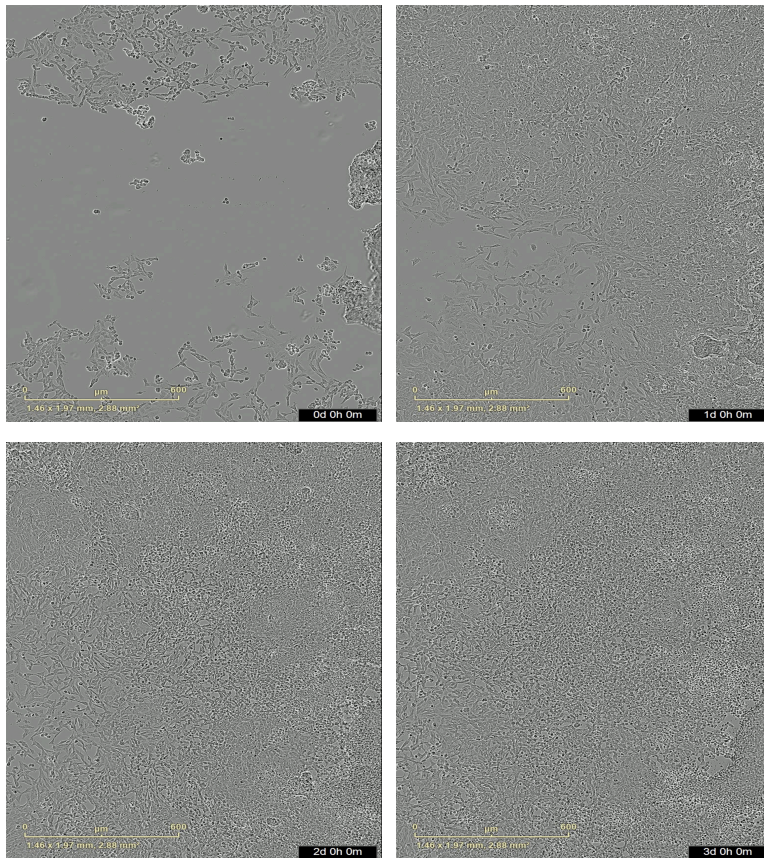


Figure 5-5. Scratch-and-heal Microscopy with KO miR-424 in MCF7 cells. All treatment conditions were plated in triplicate. Images were taken every 12 hours for 3 days. The images above are a representative sample of the dozens of images acquired.

72 hour microscopy analysis following miRNA-Control inhibition in MCF7 cells

After miR-Control inhibitor treatment, a scratch-and-heal assay was performed in order to assess the effect of miRNA inhibition on the migratory capabilities of MCF7 cells.

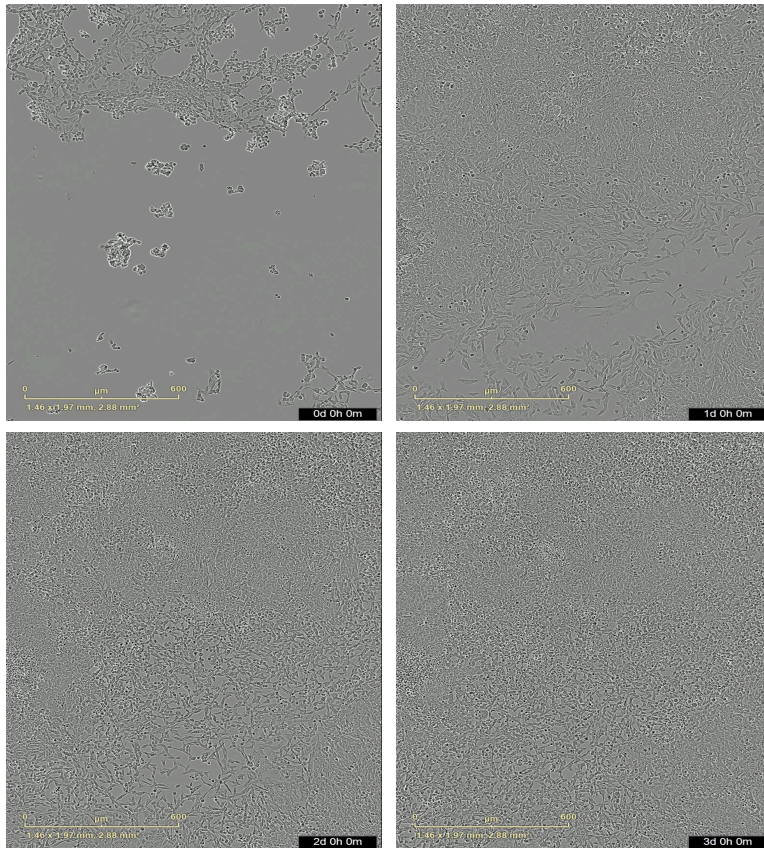


Figure 5-6. Scratch-and-heal Microscopy with miR-Control treatment in MCF7 cells. All treatment conditions were plated in triplicate. Images were taken every 12 hours for 3 days. The images above are a representative sample of the dozens of images acquired.

72 hour microscopy analysis following TE Buffer treatment in MCF7 cells

After TE buffer treatment, a scratch-and-heal assay was performed in order to assess the effect of miRNA inhibition on the migratory capabilities of MCF7 cells.

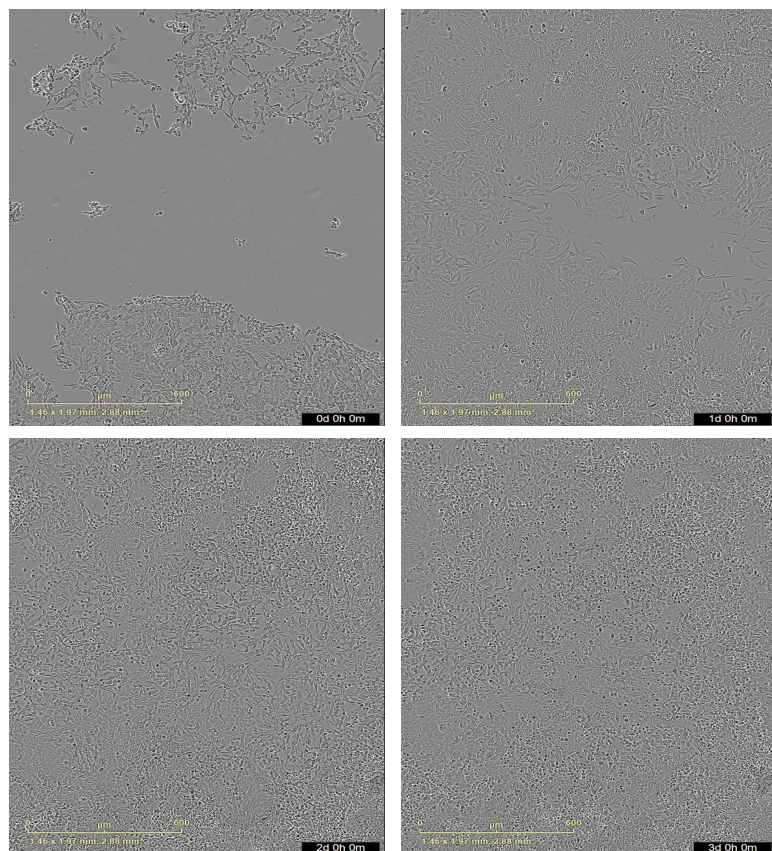


Figure 5-7. Scratch-and-heal Microscopy with TE Buffer Treatment in MCF7 cells. All treatment conditions were plated in triplicate. Images were taken every 12 hours for 3 days. The images above are a representative sample of the dozens of images acquired.

For both of the control groups, the BC cells were able to close the wound and create a single layer of cells faster than all 3 experimental conditions (Figure 5-6 & Figure 5-7). The two groups that were the slowest were KO miRNA-29c and KO miRNA-29c and KO miRNA-199a (Figure 5-3 & Figure 5-4). The microscopy results suggest that inhibiting any of these miRNA, especially miR-29c and miR-199a, decreased the ability of the MCF7 cells to “heal” from the wound. In other words, BC cells overexpress these miRNA and disrupting or decreasing their expression impedes the BC cells’ ability to migrate.

Scratch-and-heal analysis following miRNA inhibition in MCF7 cells

After miRNA-29c, 199a, 424 inhibition, (including miR-C and vehicle control TE buffer treatment) a scratch-and-heal assay was performed in order to assess the effect of miRNA inhibition on the migratory capabilities of MCF7 cells. The figure below depicts Wound Width (WW) or the distance of the gap between the top and bottom sections of cells after the scratch over 72 hours.

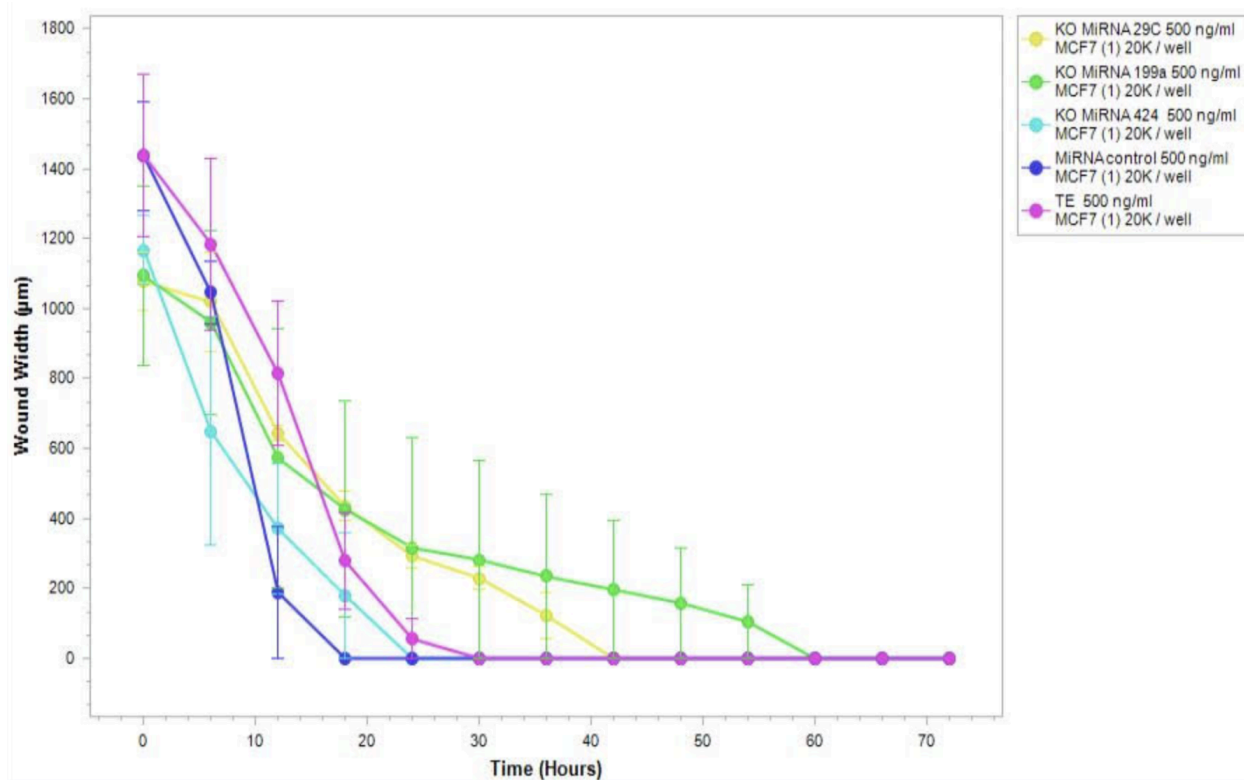


Figure 5-8. Wound Width over Time in MCF7 Cells Following miRNA Inhibition. WW measurements (in μm) are on the y axis with Time in hours on the x axis. Each dot represents 6 hours with the error bars accounting for standard deviation.

After miRNA-29c, 199a, 424 inhibition, (including miR-C and vehicle control TE buffer treatment) a scratch-and-heal assay was performed in order to assess the effect of miRNA inhibition on the migratory capabilities of MCF7 cells. The figure below highlights Wound Confluence (WC) over 72 hours. This metric assess the amount of confluent cells within the wound region.

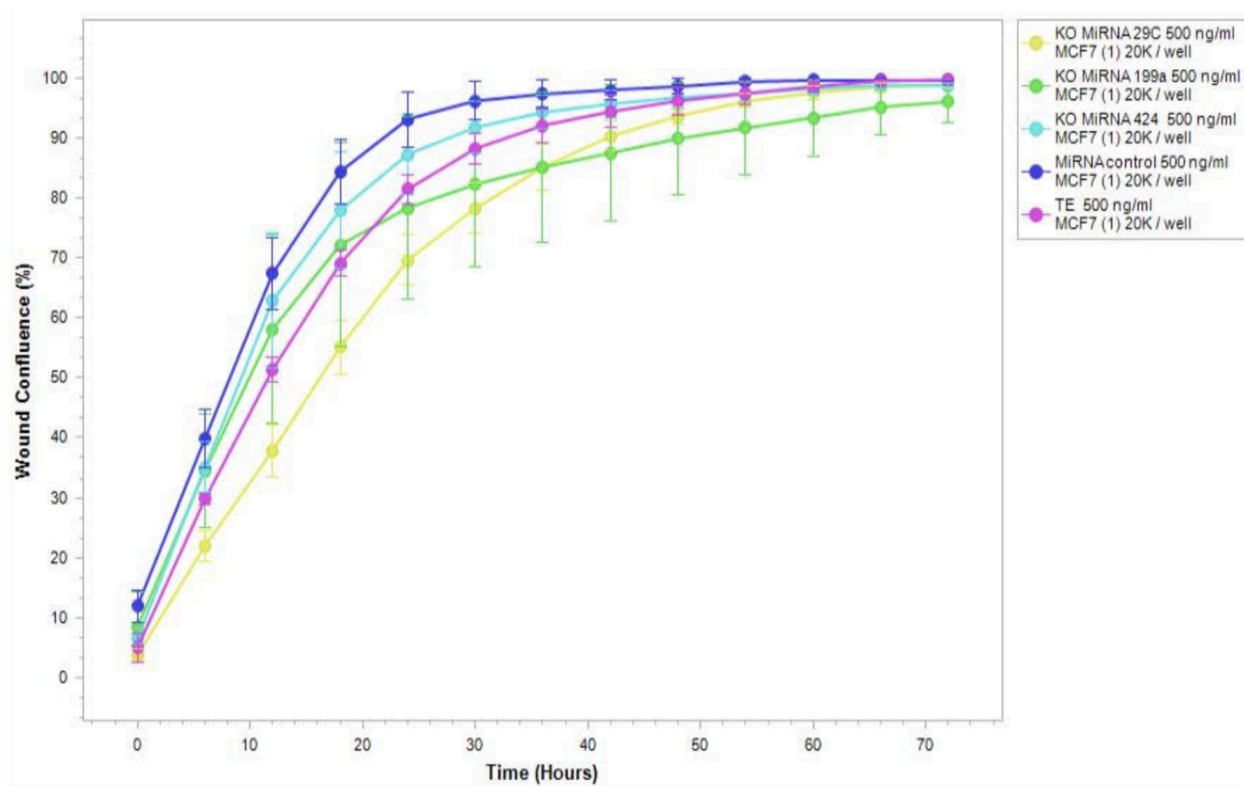


Figure 5-9. Wound Confluence over Time in MCF7 Cells Following miRNA Inhibition. WC as a percentage lies on the y axis with Time in hours on the x axis. Each dot represents 6 hours with the error bars accounting for standard deviation.

After miRNA-29c, 199a, 424 inhibition, (including miR-C and vehicle control TE buffer treatment) a scratch-and-heal assay was performed in order to assess the effect of miRNA inhibition on the migratory capabilities of MCF7 cells. The figure below illustrates Relative Wound Density (RWD) over 72 hours. RWD is the cell density in the wound area expressed relative to the cell density outside of the wound area over time.

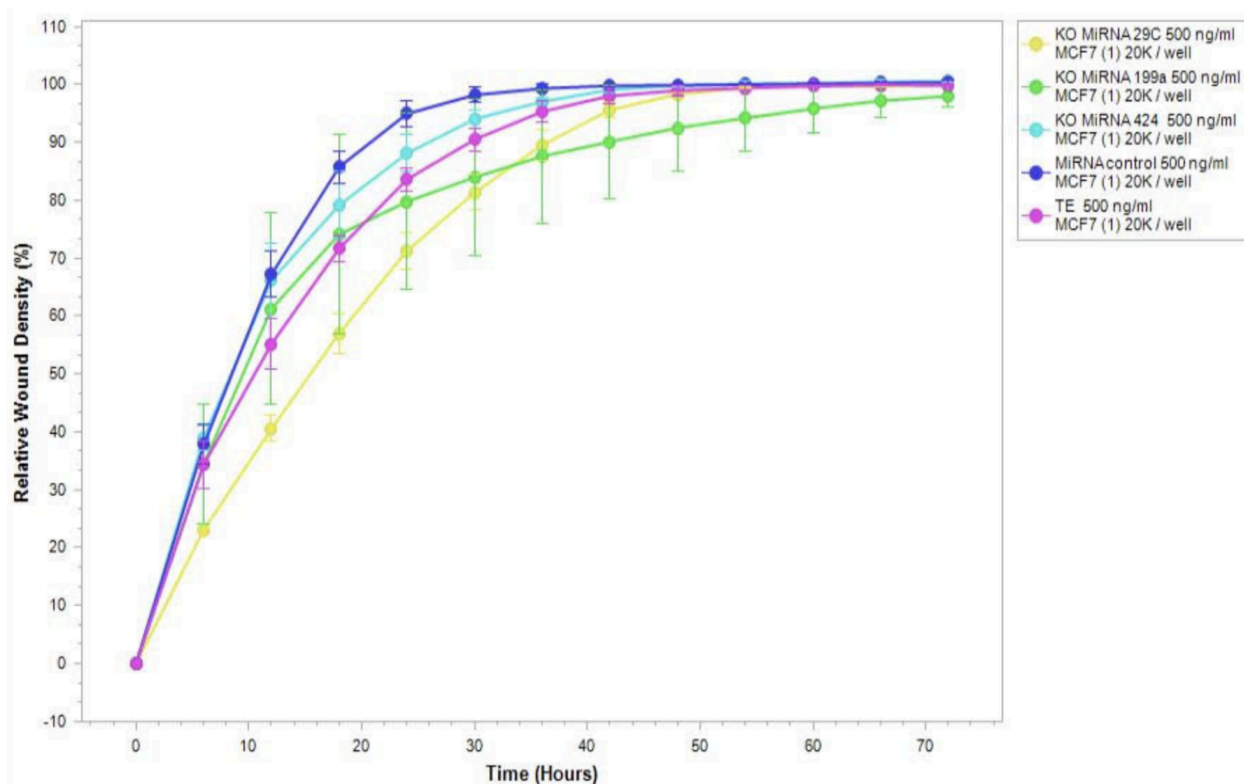


Figure 5-10. Relative Wound Density over Time in MCF7 Cells Following miRNA Inhibition. RWD as a percentage lies on the y axis with Time in hours on the x axis. Each dot represents 6 hours with the error bars accounting for standard deviation.

Ultimately, Figures 5-8~5-10 provide insight into the effects of miRNA inhibition on BC cells' ability to migrate. These results corroborate published literature outlining how miRNAs exemplify the complexity of cancer pathophysiology. Some miRNA downregulate proteins that help the cancer cell, while also turning on other signaling pathways that downregulate cancer development.

DISCUSSION:

The purpose of the scratch-and-heal assay in MCF7 cells provides some insight into the migratory behavior of BC. It is known that miRNAs can aid in migration, proliferation, and growth along with all of the other 7HC [29, 104, 105]. However, the interplay between miRNA downregulation of CCND1 and subsequent impact on migration in BC has yet to be completely elucidated.

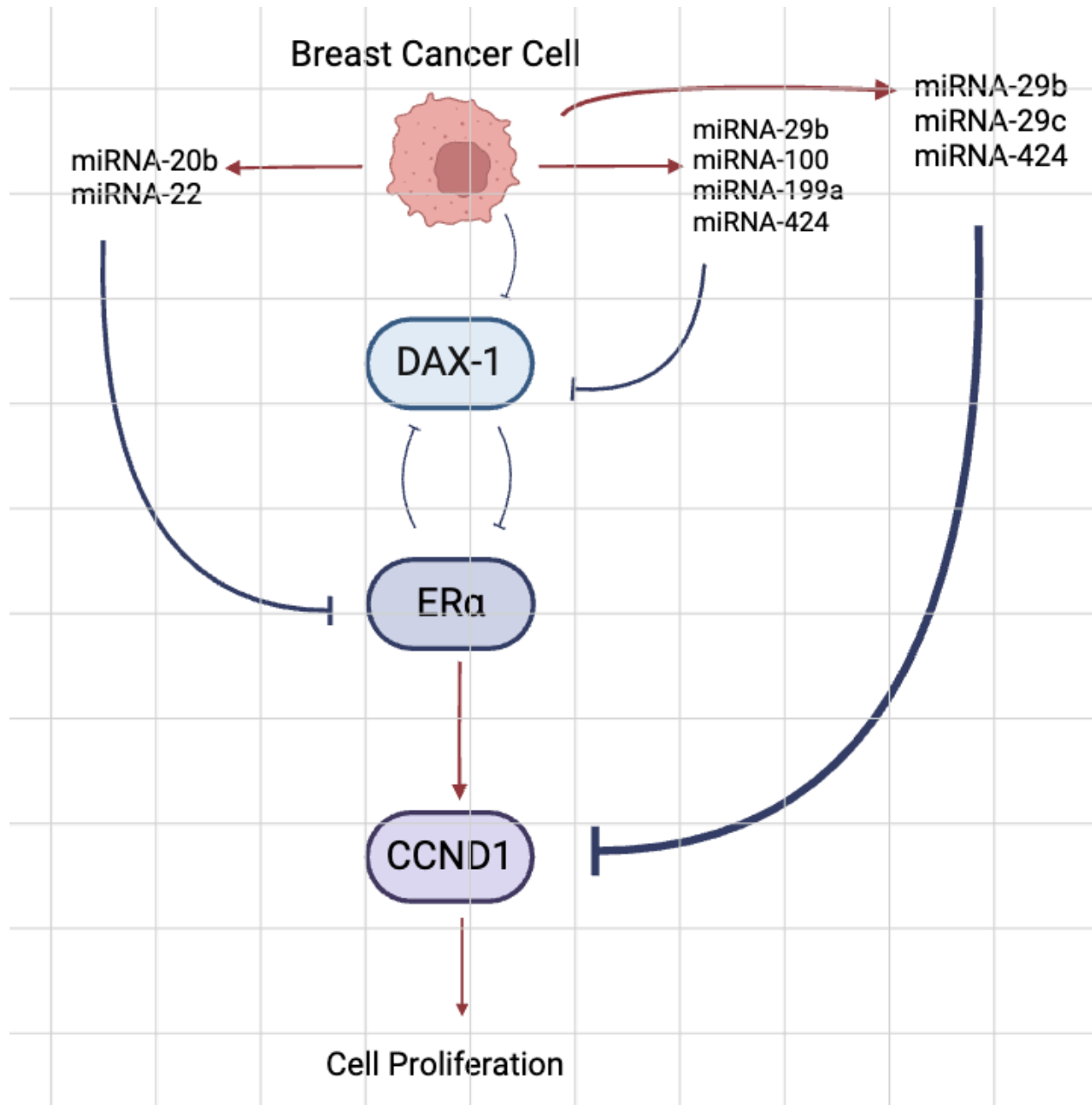
Initial microscopy images seemed to portray that inhibiting either miRNA-29c, 199a, or 424 decreased the ability of MCF7 cells to close the wound (Figure 5-3~5-7). Further computer analysis depicted much more intricate results. The first feature measured was WW. Eighteen hours after the initial scratch, the MCF7 cells with the miR-C treatment completely closed the wound (Figure 5-8). Six hours later, the KO miRNA-424 in the MCF7 cells closed the wound at 24 hours post scratch (Figure 5-8). Next, the TE buffer treatment condition, KO miRNA-29c and KO miRNA-199a were the last to “heal” from the wound (Figure 5-8). The next two metrics (WC and RWD) elicited the same order of wound healing as WW (Figure 5-9 and Figure 5-10). The data from Chapter 4 and Chapter 5 corroborates the contradictory role of miRNAs in BC development. As miRNA-29c inhibits CCND1 in BC seemingly preventing aberrant growth, the results from this chapter indicate that inhibiting miRNA-29c detrimentally modulates the ability of MCF7 cells to migrate. The same was observed for miRNA-424, however at a much lower extent. While there were varying results on the impact of miRNA-199a on CCND1 expression, it is certainly probable that regardless of CCND1 expression miRNA-199a contributes to the ability of BC cells to migrate quickly. Ultimately, both miRNA-29c and miRNA-199a contribute to the migratory abilities of MCF7 cells while miRNA-424 does not.

THESIS SUMMARY

miRNAs influence a wide range of biological processes as surveyors of genetic material. Their ability to influence mRNA and protein levels has led to vast developments in miRNA-related cancer research. However, the mechanisms for how these miRNA influence cancer potentiation have been studied much less extensively. Similarly, the role of DAX-1, an orphan nuclear hormone receptor, has been canonically illustrated as a driver of mammalian sex determination and steroidogenesis, but more recently has been identified as a modulator of cancer progression. Overall, my primary hypothesis remains that multiple miRNAs negatively regulate the expression of DAX-1 in human breast cancer cells and are not overexpressed in normal breast cells, providing another mechanism of lifting the repression of DAX-1 expression. Ultimately, the results and subsequent analysis aforementioned supports this hypothesis.

My first specific aim remained to broadly survey miRNA expression in both MCF7 and MCF10A cell lines. After completing the miRCURY LNA miRNA Focus PCR Panel Human Breast Cancer assays, 7 miRNA were repeatedly and significantly upregulated in MCF7 cells (Table 2-4). Next, specific miRNA inhibitors were used to inactivate the 7 miRNA in order to analyze the effect of miRNA inhibition on DAX-1 expression. Western blot and qPCR analysis highlighted 4 miRNA that seemingly target DAX-1 in MCF7 cells. These miRNA are: miRNA-29b, 100, 199a and 424. Additionally, future experiments such as RNAseq should be completed in order to outline the specific mechanism of action in this pathway. Results outlining the miRNA within the binding pocket of DAX-1 would strongly suggest that multiple miRNA specifically bind to DAX-1 in order to decrease DAX-1 expression as opposed to an upstream target of DAX-1. My next aim focused on investigating the effect of the same miRNA inhibition on the 2 downstream targets in the DAX-1/ER α /CCND1 axis. Quantitative PCR and western blot results provided evidence that both miRNA-20b and miRNA-22 downregulate ER α expression.

The same techniques were applied for CCND1 analysis, where miRNA-29b, 29c, and 424 were identified as inhibitors of CCND1 expression. A scratch-and-heal assay was used in order to complete my final aim: explore the impact of miRNA inhibition on the migratory capabilities of MCF7 cells. Of the 3 miRNA in question, there is only evidence suggesting miRNA-29c and miRNA-199a overexpression contributes to an increase in the migratory tendencies of MCF7 cells. The role miRNA upregulation plays in the aforementioned DAX-1/ER α /CCND1 axis in BC is summarized in Figure 6-1 below.



Created with BioRender.com

Figure 6-1. Diagram of miRNA Modulation of the DAX-1/ER α /CCND1 axis in MCF7 cells. The blue lines with the perpendicular ends indicate inhibition while the red arrows represent activation.

In addition to their role as drivers of BC development, miRNAs have also been elucidated to be excellent biomarkers. Biomarkers are measurable indicators of biological processes [106]. In cancer, biomarkers can assist in early detection, diagnosis, prognosis, and predicting therapeutic response [107]. Furthermore, research has suggested using urinary miRNA levels as biomarkers is 98.6% effective at diagnosing BC compared to healthy controls [108]. In this specific study 4 miRNA (including miR-424) were used to differentiate between a BC and control patients. Additional studies have explored using urinary miRNA levels with similar degrees of success [109, 110, 111]. Along the same lines, circulatory miRNAs (easily detectable via blood draw) have also been identified as accurate indicators of BC diagnosis [112, 113]. MiRNA-106a, the only previously known miRNA that targets DAX-1 in BC, has also been described as a diagnostic biomarker in BC [114]. By increasing the amount of known biomarkers and also identifying their molecular targets, clinicians will be better equipped to accurately, and inexpensively treat BC patients as quickly as possible.

In summation, the work in this thesis serves two purposes. First, to illustrate the complexity and often dual role of miRNA dysregulation in BC pathogenesis. Despite extensive research outlining the ER α /CCND1 relationship in BC, the mechanisms behind the role of DAX-1 in this pathway has been the subject of more recent analysis. In conjunction, by understanding how miRNAs interact with transcription factors in BC, clinicians will be better equipped to treat BC patients. The second purpose of this body of work remains to shed light on additional miRNAs that could be used as BC biomarkers. As rates of BC continue to increase, detecting BC as early as possible has never been more paramount. By quickly analyzing a urine sample or a blood draw, healthcare professionals can accurately and inexpensively diagnose BC more effectively than mammography. This practice is vital for future BC patients in order to

prevent disease progression and eventual metastasis. However, optimizing miRNA panels as biomarkers is even more crucial to international and global communities who are not able to access or pay for preventative mammograms. Ultimately, more patients will be diagnosed faster and ostensibly cured as more research is completed exemplifying the importance of miRNA-driven tumorigenesis.

References

1. Feng, Yi Xiao., et al. "Breast cancer development and progression: Risk factors, cancer stem cells, signaling pathways, genomics, and molecular pathogenesis." *Genes & Diseases*. 2018. 5(2): 77-106.
2. Gasco, M., et al. "The p53 pathway in breast cancer." *Breast Cancer Research and Treatment*. 2002. 4(2): 70-76.
3. von Lintig, F.C. et al. "Ras activation in human breast cancer." *Breast Cancer Research and Treatment*. 2000. 62(1): 51-62.
4. Larsen, M. et al. "Hereditary Breast Cancer: Clinical, Pathological and Molecular Characteristics." *Breast Cancer: Basic and Clinical Research*. 2014. 8: 145-155.
5. Łukasiewicz, S. et al. "Breast Cancer—Epidemiology, Risk Factors, Classification, Prognostic Markers, and Current Treatment Strategies—An Updated Review." *Cancers*. 2021. 13(17): 4287.
6. Ramón y Cajal, T. et al. "Mammographic density and breast cancer in women from high risk families." *Breast Cancer Research*. 2015. 17(93)
7. Geiger, AM., et al. "A Population-Based Study of Bilateral Prophylactic Mastectomy Efficacy in Women at Elevated Risk for Breast Cancer in Community Practices." *Arch Intern Med*. 2005. 165(5): 516–520.
8. Picon-Ruiz, M., et al. "Obesity and adverse breast cancer risk and outcome: Mechanistic insights and strategies for intervention." *CA: A Cancer Journal for Clinicians*. 2017. 96(5): 378-397.
9. Gaudet, M. et al. "Risk factors by molecular subtypes of breast cancer across a population-based study of women 56 years or younger." *Breast Cancer Research and Treatment*. 2011. 130: 587-597.
10. Lakhani, S. et al. *WHO Classification of Tumours of the Breast*. 4th ed. IARC Press; Lyon, France: 2012.
11. "Breast Cancer Staging." *Breast Cancer Surgery. American College of Surgeons*. 2024.
12. Herlevic V. et al. "Breast cancer outcomes in a population with high prevalence of obesity." *Journal of Surgical Research*. 2015. 198(2). 371-376..
13. Conde, I. et al. "DAX-1 expression in human breast cancer: comparison with estrogen ER- α , ER- β , and androgen receptor status." *Breast Cancer Research and Treatment*. 2004. 6(140).
14. Reutens, AT. et al. "Clinical and functional effects of mutations in the DAX-1 gene in patients with adrenal hypoplasia congenita." *J Clin Endocrinol Metab*. 1999. 84(2). 504-511.
15. Sukumaran, A. "Duplication of dosage sensitive sex reversal area in a 46, XY patient with normal sex determining region of Y causing complete sex reversal." *J Pediatr Endocrinol Metab*. 2013. 26(7-8). 775-779.
16. Kumar, R. and Thompson, B. "The structure of the nuclear hormone receptors." *Steroids*. 1999. 64(5): 310-319.

17. Mullican, S. et al. "The Orphan Nuclear Receptors at Their 25th year Reunion." *Journal of Molecular Endocrinology*. 2013. 51(3): 115-140.
18. Dishington, Erin. "The role of orphan nuclear receptor DAX-1 (NR0B1) in human breast cancer cells: expression, proliferation and metastasis." 2017. *University of San Francisco Library*. 269.
19. Beltran Valencia, Roxana Valeria. "Regulation of proliferation, apoptosis, and metastasis in prostate cancer cells by DAX-1 (NR0B1)- an androgen-induced orphan nuclear receptor." (2017). Master's Theses. 248.
20. Pu, M. et al. "Regulatory network of miRNA on its target: coordination between transcriptional and post-transcriptional regulation of gene expression." *Cellular and Molecular Life Sciences*. 2019. 76: 441-451.
21. Yang, A. et al. "AGO-bound mature miRNAs are oligouridylated by TUTs and subsequently degraded by DIS3L2." *Nature Communications*. 2020. 11(2765).
22. Winter, J. et al. "Many roads to maturity: microRNA biogenesis pathways and their regulation." *Nat Cell Biol*. 2009. 11: 228–234.
23. Kehl, T. et al. "About miRNAs, miRNA seeds, target genes and target pathways." *Oncotarget*. 2017. 8(63): 107167-107175.
24. Babashah, S. and Soleimani, M. "The oncogenic and tumor suppressive roles of microRNAs in cancer and apoptosis." *European Journal of Cancer*. 2011. 47(8): 1127-1137.
25. Singh, R. and Mo, Y. "Role of miRNAs in breast cancer." *Cancer Biology & Therapy*. 2013. 14(3): 201-212.
26. Liu, C. et al. "MiRNA-106a promotes breast cancer progression by regulating DAX-1." *European Review for Medical and Pharmacological Sciences*. 2019. 23(4): 1574-1583.
27. Tong, S. et al. "microRNA-181 promotes prostate cancer cell proliferation by regulating DAX-1 expression." *Experimental and Therapeutic Medicine*. 2014. 8(4): 1296-1300.
28. Fouad, Y.A. and Aanei, C. "Revisiting the hallmarks of cancer." *Am J Cancer Res*. 2017. 7(5):1016-1036.
29. Nurzadeh, M. et al. "A comprehensive review on oncogenic miRNAs in breast cancer." *J Genet*. (2021). 100(15).
30. Yokoi, A., et al. "Integrated extracellular microRNA profiling for ovarian cancer screening." *Nature Communications*. 2018.
31. Avery-Kiejda, K., et al. "Decreased expression of key tumour suppressor microRNAs is associated with lymph node metastases in triple negative breast cancer." *BMC Cancer*. 2014.
32. Zhu, M., et al. "Genomic Profiling of mouse mammary tumor models identifies miRNA signatures associated with mammary tumor lineage (mammary normal and tumors in different mice strains." *NCBI*. 2011.
33. Yan, M. "Comparative microRNA profiling of sporadic and BRCA1 associated basal-like breast cancers." *NCBI*. 2014.

34. Hsien-Lee, C., et al. "MicroRNA-regulated protein-protein interaction networks and their functions in breast cancer." *Int J Mol Sci.* 2013.
35. Usuba, W., et al. "Circulating miRNAs panels for specific and early detection in bladder cancer." *Cancer Science.* 2019.
36. Yamamoto, Y., et al. "Highly Sensitive Circulating MicroRNA Panel for Accurate Detection of Hepatocellular Carcinoma in Patients with Liver Disease." *Hepatol Communications.* 2019.
37. Biagioni, F., et al. "miR-10b*, a master inhibitor of the cell cycle, is down-regulated in human breast tumours." *EMBO Mol Med.* 2012.
38. Blenkiron, C., et al. "MicroRNA expression profiling of human breast cancer identifies new markers of tumor subtype." *Genome Biol.* 2007.
39. Bacci, M., et al. "Reprogramming of Amino Acid Transporters to Support Aspartate and Glutamate Dependency Sustains Endocrine Resistance in Breast Cancer." *Cell Press.* 2019.
40. Shen, J., et al. "BK5 ATF3-induced mammary tumors compared to normal mammary glands." *NCBI.* 2021.
41. Lesurf, R., et al. "Molecular Features of Subtype-Specific Progression from Ductal Carcinoma In Situ to Invasive Breast Cancer." *Cell Rep.* 2016.
42. Memoli, D. "Estrogen receptor beta inhibits cholesterol biosynthesis through overexpression of mir-181a-5p in Triple Negative Breast Cancer." *BioStudies Array Express.* 2020.
43. Gravggaard, K., et al. "The miRNA-200 family and miRNA-9 exhibit differential expression in primary versus corresponding metastatic tissue in breast cancer." *Breast Cancer Research Treatment.* 2012.
44. Mattie, M., et al. "Optimized high-throughput microRNA expression profiling provides novel biomarker assessment of clinical prostate and breast cancer biopsies." *Molecular Cancer BioMed Central.* 2006.
45. Tanic, M., et al. "MicroRNA expression signatures for the prediction of BRCA1/2 mutation-associated hereditary breast cancer in paraffin-embedded formalin-fixed breast tumors." *Int J Cancer.* 2015.
46. Lu, J., et al. "MicroRNA expression profiles classify human cancers." *Nature.* 2005.
47. Kumar, LD., et al. "MicroRNA profiling in different types, grades and stages of breast cancer." *NCBI.* 2020.
48. Romero-Cordoba, S., et al. "Loss of function of miR-342-3p results in MCT1 over-expression and contributes to oncogenic metabolic reprogramming in triple negative breast cancer." *Scientific Reports.* 2018.
49. Enerly, E., et al. "miRNA-mRNA integrated analysis reveals roles for miRNAs in primary breast tumors." *Plos One.* 2011.

50. Buffa, F., et al. "microRNA-associated progression pathways and potential therapeutic targets identified by integrated mRNA and microRNA expression profiling in breast cancer." *Cancer Res.* 2011.
51. Schrauder, M., et al. "Circulating micro-RNAs as potential blood-based markers for early stage breast cancer deduction." *PLoS One.* 2012.
52. Feliciano, A., et al. "miR-125b acts as a tumor suppressor in breast tumorigenesis via its novel direct targets ENPEP, CK2- α , CCNJ, and MEGF9." *Plos One.* 2013.
53. Hannafon, B., et al. "Expression of microRNA and their gene targets are dysregulated in preinvasive breast cancer." *Breast Cancer Research.* 2011.
54. Gao, L., et al. "Comprehensive Transcriptomic Analysis Reveals Dysregulated Competing Endogenous RNA Network in Endocrine Resistant Breast Cancer Cells." *Front Oncology.* 2020.
55. Zhao, X., et al. "miR-665 expression predicts poor survival and promotes tumor metastasis by targeting NR4A3 in breast cancer." *Cell Death Discussion.* 2019.
56. Lee, C., et al. "MicroRNA-regulated-protein-protein interaction networks and their functions in breast cancer." *Int J Mol Sci.* 2013.
57. Iizuka, D., et al. "Aberrant microRNA expression in radiation-induced rat mammary cancer: the potential role of miR-194 overexpression in cancer cell proliferation." *NCBI.* 2013.
58. Mohd, A., et al. "DK2, a newly synthesized chalcone, induced apoptosis and differential expression profiles of miRNA and mRNA on breast cancer MCF-7 cell line." *NCBI.* 2020.
59. Chan, M., et al. "Identification of circulating microRNA signatures for breast cancer detection." *Clinical Cancer Research.* 2013.
60. Wightman B., et al. "Posttranscriptional regulation of the heterochronic gene lin-14 by lin-4 mediates temporal pattern formation in *C. elegans*." *Cell.* 1993. 75(5):855-62.
61. Stark A., et al. "Identification of *Drosophila* MicroRNA targets." *PLoS Biol.* 2003. 1(3):E60.
62. Lagos-Quintana M., et al. "Identification of novel genes coding for small expressed RNAs." *Science.* 2001. 294(5543):853-8.
63. Lau NC., et al. "An abundant class of tiny RNAs with probable regulatory roles in *Caenorhabditis elegans*." *Science.* 2001. 294(5543):858-62.
64. Rodriguez A., et al. "Identification of mammalian microRNA host genes and transcription units." *Genome Res.* 2004. 14(10A):1902-10.
65. Cullen, BR. "Transcription and processing of human microRNA precursors." *Mol Cell.* 2004. 16(6):861-5.
66. Tanzer A. and Stadler PF. "Molecular evolution of a microRNA cluster." *J Mol Biol.* 2004. 339(2):327-35.
67. Concepcion CP., et al. "The microRNA-17-92 family of microRNA clusters in development and disease." *Cancer J.* 2012. 18(3):262-7.

68. Nunes DN., et al. "Synchronous down-modulation of miR-17 family members is an early causative event in the retinal angiogenic switch." *Proc Natl Acad Sci USA*. 2015. 112(12):3770-5.
69. Li JY., et al. "Differential distribution of miR-20a and miR-20b may underly metastatic heterogeneity of breast cancers." *Asian Pac J Cancer Prev*. 2012.13(5):1901-6.
70. Wang C., et al. "A combined approach identifies three mRNAs that are down-regulated by microRNA-29b and promote invasion ability in the breast cancer cell line MCF-7." *J Cancer Res Clin Oncol*. 2012. 138(12):2127-36.
71. Jiang H., et al. "Diverse roles of miR-29 in cancer (review)." *Oncol Rep*. 2014. 31(4):1509-16.
72. Yan B., et al. "The role of miR-29b in cancer: regulation, function, and signaling." *Onco Targets Ther*. 2015. 3(8):539-48.
73. Riedstra, Caroline P., "Examination of Methylation Status and Occupancy of DNA Methylation Modifying Proteins on Regulatory Regions of the DAX-1 Gene" (2021). *Master's Theses*. 1393.
74. Eniafe J., and Jiang S. "MicroRNA-99 family in cancer and immunity." *Wiley Interdiscip Rev RNA*. 2021. 12(3):e1635.
75. Webb P., et al. "The estrogen receptor enhances AP-1 activity by two distinct mechanisms with different requirements for receptor transactivation functions." *Mol Endocrinol*. 1999. 13(10):1672-85.
76. Ali, S., and Coombes, R.C. "Estrogen Receptor Alpha in Human Breast Cancer: Occurrence and Significance." *J Mammary Gland Biol Neoplasia*. 2000. 5:271–281
77. Zhang, H., et al. "DAX-1 Functions as an LXXLL-containing Corepressor for Activated Estrogen Receptors*." *Genes: Structure and Regulation*. 2000. 275(51): 39855-59.
78. Diehl, J. A. "Cycling to Cancer with Cyclin D1." *Cancer Biology & Therapy*. 2002. 1(3):226–231.
79. Zwijssen RM., et al. "CDK-independent activation of estrogen receptor by cyclin D1." *Cell*. 1997. 88(3):405-15.
80. Wang, J. et al. "miRNA-194 predicts favorable prognosis in gastric cancer and inhibits gastric cancer cell growth by targeting CCND1." *FEBS OpenBio*. 2021. 11(7):1814-26.
81. Eeckhoutte J., et al. "A cell-type-specific transcriptional network required for estrogen regulation of cyclin D1 and cell cycle progression in breast cancer." *Genes Dev*. 2006. 20(18):2513-26.
82. Castellano L., et al. "The estrogen receptor-alpha-induced microRNA signature regulates itself and its transcriptional response." *Proc Natl Acad Sci USA*. 2009. 106(37):15732-7.
83. Xiong J., et al. " An estrogen receptor alpha suppressor, microRNA-22, is downregulated in estrogen receptor alpha-positive human breast cancer cell lines and clinical samples." *FEBS J*. 2010. 277(7):1684-94.
84. Cochrane DR., et al. "MicroRNAs link estrogen receptor alpha status and Dicer levels in breast cancer." *Horm Cancer*. 2010. 1(6):306-19.

85. Pandey DP., and Picard D. "miR-22 inhibits estrogen signaling by directly targeting the estrogen receptor alpha mRNA." *Mol Cell Biol.* 2009. 29(13):3783-90.
86. Zhou W., et al. "MicroRNA-20b promotes cell growth of breast cancer cells partly via targeting phosphatase and tensin homologue (PTEN)." *Cell Biosci.* 2014. 4(1):62.
87. Huang ZP., and Wang DZ. "miR-22 in cardiac remodeling and disease." *Trends Cardiovasc Med.* 2014. 24(7):267-72.
88. Gao S., et al. "microRNA-Dependent Modulation of Genes Contributes to ESR1's Effect on ER α Positive Breast Cancer." *Front Oncol.* 2020. 10:753.
89. Jiang G., et al. "Cooperativity of co-factor NR2F2 with Pioneer Factors GATA3, FOXA1 in promoting ER α function." *Theranostics.* 2019. 9(22):6501-6516.
90. Fu, X.Y., et al. "FOXA1 upregulation promotes enhancer and transcriptional reprogramming in endocrine-resistant breast cancer." *PNAS.* 2019. 116(52): 26823-34.
91. Hurtado A., et al. "FOXA1 is a key determinant of estrogen receptor function and endocrine response." *Nat Genet.* 2011. 43(1):27-33.
92. Xie H., et al. "MicroRNA-100 inhibits breast cancer cell proliferation, invasion and migration by targeting FOXA1." *Oncol Lett.* 2021. 22(6):816.
93. Zhang NS., et al. "MicroRNA-29 family functions as a tumor suppressor by targeting RPS15A and regulating cell cycle in hepatocellular carcinoma." *Int J Clin Exp Pathol.* 2017. 10(7):8031-8042.
94. Linsley PS., et al. "Transcripts targeted by the microRNA-16 family cooperatively regulate cell cycle progression." *Mol Cell Biol.* 2007. Mar;27(6):2240-52.
95. Xie D., et al. "MicroRNA-424 serves an anti-oncogenic role by targeting cyclin-dependent kinase 1 in breast cancer cells." *Oncol Rep.* 2018. 40(6):3416-3426.
96. Wang C., et al. "A combined approach identifies three mRNAs that are down-regulated by microRNA-29b and promote invasion ability in the breast cancer cell line MCF-7." *J Cancer Res Clin Oncol.* 2012. 138(12):2127-36.
97. Lehn S., et al. "Down-regulation of the oncogene cyclin D1 increases migratory capacity in breast cancer and is linked to unfavorable prognostic features." *Am J Pathol.* 2010. 177(6):2886-97.
98. Zhang D., et al. "Hypoxia-induced miR-424 decreases tumor sensitivity to chemotherapy by inhibiting apoptosis." *Cell Death Dis.* 2014. 5(6).
99. Greenburg G., and Hay, ED. "Epithelia suspended in collagen gels can lose polarity and express characteristics of migrating mesenchymal cells." *J Cell Biol.* 1982. 95(1):333-9.
100. Zeisberg M., and Neilson, EG. "Biomarkers for epithelial-mesenchymal transitions." *J Clin Invest.* 2009. 119(6):1429-37.
101. Ahmadiankia N., et al. "Berberine suppresses migration of MCF-7 breast cancer cells through down-regulation of chemokine receptors." *Iran J Basic Med Sci.* 2016. 19(2):125-31.

102. Kauanova S., et al. "The Frequent Sampling of Wound Scratch Assay Reveals the "Opportunity" Window for Quantitative Evaluation of Cell Motility-Impeding Drugs." *Front Cell Dev Biol.* 2021. 9:640972.
103. McSherry, E.A., et al. "Breast cancer cell migration is regulated through junctional adhesion molecule-A-mediated activation of Rap1 GTPase." *Breast Cancer Res.* 2011. 13(R31).
104. Peng Y, and Croce, CM. "The role of MicroRNAs in human cancer." *Signal Transduct Target Ther.* 2016. 1:15004.
105. Chakraborty A., et al. "miRNAs: Potential as Biomarkers and Therapeutic Targets for Cancer." *Genes.* 2023. 14(7):1375.
106. Strimbu K., and Tavel, JA. "What are biomarkers?" *Curr Opin HIV AIDS.* 2010. 5(6):463-6.
107. Sarhadi VK., and Armengol G. "Molecular Biomarkers in Cancer." *Biomolecules.* 2022. 12(8):1021.
108. Hirschfeld M., et al. "Urinary Exosomal MicroRNAs as Potential Non-invasive Biomarkers in Breast Cancer Detection." *Mol Diagn Ther.* 2020. 24(2):215-232.
109. Erbes T., et al. "Feasibility of urinary microRNA detection in breast cancer patients and its potential as an innovative non-invasive biomarker." *BMC Cancer.* 2015. 15:193.
110. Ando, W., et al. "Novel breast cancer screening: combined expression of miR-21 and MMP-1 in urinary exosomes detects 95% of breast cancer without metastasis." *Sci Rep.* 2019. 9:13595.
111. Gasparri ML., et al. "Beyond circulating microRNA biomarkers: Urinary microRNAs in ovarian and breast cancer." *Tumor Biology.* 2017. 39(5).
112. Kassem NM., et al. "Circulating miR-34a and miR-125b as Promising non Invasive Biomarkers in Egyptian Locally Advanced Breast Cancer Patients." *Asian Pac J Cancer Prev.* 2019. 20(9):2749-2755.
113. Nguyen THN., et al. "Panels of circulating microRNAs as potential diagnostic biomarkers for breast cancer: a systematic review and meta-analysis." *Breast Cancer Res Treat.* 2022. 196(1):1-15.
114. Li M., et al. "Circulating microRNAs from the miR-106a-363 cluster on chromosome X as novel diagnostic biomarkers for breast cancer." *Breast Cancer Res Treat.* 2018. 170(2):257-270.